Overexpression of Membrane Proteins in Saccharomyces cerevisiae for Structural and Functional Studies: A Focus on the Rabbit Ca2+-ATPase Serca1a and on the Yeast Lipid "Flippase" Complex Drs2p/Cdc50p

Cédric Montigny, Hassina Azouaoui, Aurore Jacquot, Marc Le Maire, Christine Jaxel, Philippe Champeil, Guillaume Lenoir

Chapter 6
Overexpression of Membrane Proteins in *Saccharomyces cerevisiae* for Structural and Functional Studies: A Focus on the Rabbit Ca^{2+}-ATPase Serca1a and on the Yeast Lipid "Flippase" Complex Drs2p/Cdc50p

Cédric Montigny, Hassina Azouaoui, Aurore Jacquot, Marc le Maire, Christine Jaxel, Philippe Champeil and Guillaume Lenoir

6.1 Introduction

The so-called baker's yeast, *Saccharomyces cerevisiae,* has been used for centuries by humans to produce food and beverages like bread and beer (or wine). Since its complete genome sequencing in 1996 (Goffeau et al. 1996), we know that it contains about 6,000 genes and that about 25 % of them encode putative membrane proteins (MPs). For comparison, human cells contain about 25,000 genes and the same proportion of putative MPs as in yeast (Lander et al. 2001; Venter et al. 2001). Yeast cells share with human cells similar protein synthesis mechanisms, maturation machinery, and membrane-trafficking pathways. As a result, *S. cerevisiae* is probably the best characterized and the most widespread model for studying eukaryotic cell biology.

Genetic engineering of *S. cerevisiae* started in the 1970s with a description of homologous recombination mechanisms, discovery of numerous yeast plasmids (Gunge 1983), and the development of recombinant DNA technologies. This led to its use as a powerful biotechnology tool for protein overexpression, prominent examples being overproduction of recombinant human insulin precursors in 1987 (Novolin R®, Novo Nordisk) or production of the first effective vaccine against human viral infections by hepatitis B (Diers et al. 1991; McAleer et al. 1984). Due to the simplicity of its genome and its ability to perform homologous recombination,

Cédric Montigny and Hassina Azouaoui contributed equally to this work.

G. Lenoir (✉) · C. Montigny · H. Azouaoui · A. Jacquot · M. le Maire · C. Jaxel · P. Champeil
Laboratory of Membrane Proteins, Institute of Biology and Technology of Saclay, UMR-CNRS 8221, Centre for Nuclear Studies and Université Paris-Sud, Gif-sur-Yvette, France
e-mail: guillaume.lenoir@cea.fr

I. Mus-Veteau (ed.), *Membrane Proteins Production for Structural Analysis,*
DOI 10.1007/978-1-4939-0662-8_6,

S. cerevisiae genetic manipulation is now straightforward (Wach 1996). Isolation of genes and design of disruption cassettes allowed obtaining thousands of mutants that are available for the international community (EUROpean Saccharomyces Cerevisiae ARchive for Functional Analysis data bank, http://web.uni-frankfurt.de/fb15/mikro/euroscarf/). Whole genome and proteome information are available on the Saccharomyces Genome Database website (http://www.yeastgenome.org/).

Since the 1990s, *S. cerevisiae* has been used as a heterologous expression system for MPs (for review, Grisshammer and Tate 1995). Yet, despite intense efforts, only a limited amount of high-resolution structures of yeast-expressed eukaryotic MPs have been solved so far (see Table 6.1; White 2013). There is still a long way to go but recent technical advances should help overcome barriers in MP structure determination (Carpenter et al. 2008; Lee and Stroud 2010). Our goal in this chapter is not to give an exhaustive inventory of yeast expression systems, which have been excellently reviewed elsewhere (Britton et al. 2011), but rather to focus on systems used or specifically developed for eukaryotic MP overexpression and which led to the determination of high-resolution structures.

6.2 *S. cerevisiae* as a Host for Heterologous Expression of MPs

S. cerevisiae seems to be an appropriate expression system for large-scale production of MPs. This organism is able to perform most of the eukaryotic posttranslational modifications such as disulfide bond formation, glycosylation, and proteolytic maturation. From a cell-biological point of view, yeast contains almost all internal organelles that are found in mammalian cells (instead of lysosomes, they contain a related compartment called vacuole, which is also found in plants), and expressed MPs may be targeted to these specific membranes (Zimmermann et al. 2011; Weis et al. 2013). As mentioned in the introduction, molecular biology techniques are well documented and fairly simple compared to other eukaryotic expression systems; thus, this organism is well suited for cloning and mutagenesis using classical molecular biology tools. In addition, yeasts are easy to cultivate; growth conditions are well described and scaling up cultures from small volumes to some tenth of liters is relatively straightforward. However, it is important to be aware that *S. cerevisiae* is not a perfect model for mammalian cells. Differences in membrane lipid composition or in the glycosylation machinery may turn out to be critical for MP folding and function. As an example, *N*-glycan structures generated in the Golgi of *S. cerevisiae* are made exclusively of one sugar type, mannose, while mammalian *N*-glycans are much more diverse.

Two main cloning methods have been used for protein overexpression in yeast. The target gene may be cloned on an episomal plasmid that replicates separately from the yeast chromosome; in this case, the number of plasmids per cells may be very low, and therefore selection pressure has to be maintained tightly to prevent plasmid loss during prolonged culture of the cells. Another method consists in taking advantage of the homologous recombination ability of *S. cerevisiae,* by intro-

Table 6.1 Integral eukaryotic membrane proteins for which crystal structures have been obtained after expression in *S. cerevisiae*

Name of the protein	ATP synthase	Ca^{2+}-ATPase	Monoamine oxidase A	H^+-PPase	CAAX protease Ste24p	PiPT	Vcx1p
General description							
Function	ATP biosynthesis in mitochondria	Ca^{2+} transport into sarco(endo)plasmic reticulum	Deamination of several neurotransmitters	Pyrophosphate-dependent proton translocation in vacuoles	Maturation of yeast mating pheromone a-factor	Phosphate-protons symporter	Vacuolar Ca^{2+}/H^+ exchanger
Source	*S. cerevisiae*	Rabbit	Rat Human	*Vigna radiata* (Mung bean)	*Saccharomyces mikatae*	*Piriformospora indica* (Fungi)	*S. cerevisiae*
Number of TM	20 (decamer of 2)	10	2 (dimer of 1)	16	7	8	11
References	Stock et al. 1999	Jidenko et al. 2005; Marchand et al. 2008	Ma et al. 2004a, b Son et al. 2008	Lin et al. 2012	Pryor et al. 2013	Pedersen et al. 2013	Waight et al. 2013
Expression							
Vector	–	pYeDP60	YEp51	pYES2	pSGP46	p423-GAL1	p423-GAL1
Promoter	–	*CYC1-GAL10*	*GAL10*	*GAL1*	*ADH2*	*GAL1*	*GAL1*
Strain	*Natural source*	W303.1b [*GAL4*]	BJ2168	BJ2168	BJ5460	DSY-5	DSY-5
Extraction and purification							
Lysis process	Glass beads and bead beater	Glass beads and planetary shaker	Zymolyase and sonication	Lyticase and homogenizer	Freeze/thaw cycles and French press	Glass beads and bead beater	Glass beads and bead beater
Tag position	–	C-terminus	N-terminus	C-terminus	C-terminus	N- and C-terminus	N- and C-terminus
Tag nature	–	BAD	His_6	His_6	IgG binding site	His_6	His_6
Detergent	DDM	DDM	FC-12	DDM	DDM+$C_{12}E_7$	DDM	DDM
Purification steps	Q-Sepharose and Sephacryl 300	Streptavidine-Sepharose and TSK 3000 SW	Ni^{2+}-NTA	Ni^{2+}-NTA	IgG Sepharose 6 and high load 16/60 Superdex 200	Ni^{2+}-NTA	TALON Co^{2+}
Yield, mg/L of culture	–	0.3–1	10 –	1.2	0.6	3–5	-

Table 6.1 (continued)

Name of the protein	ATP synthase	Ca^{2+}-ATPase	Monoamine oxidase A		H^+-PPase	CAAX protease Ste24p	PiPT	Vcx1p
Crystallization								
Method	Microbatch in paraffin oil	Hanging/sitting drops	Hanging drops	Sitting drops	Hanging drops	Sitting drops	Hanging drops	Hanging drops (lipidic cubic phase)
Detergent	DDM	$C_{12}E_8$	FC-12, APO 10		DDM	$C_{12}E_7$	NG/DDM or DM	DDM
Lipids	–	DOPC	–		–	–	–	Monoolein
Ligands	–	Ca^{2+} and ATP analogs	–	Inhibitors	Substrate analog	–	–	Ca^{2+} and Mn^{2+}
Resolution, Å	3.9	3.0–3.5	3.2	2.2	2.35	3.1	2.7/4–6	2.3
PDB entry code	1QO1	–	1O5W	2Z5X	4AO1	4IL3	4JO5/-	4K1C

ducing the gene of interest on a plasmid that will subsequently be integrated into the yeast genome (Wach 1996; Decottignies et al. 1998; Nagy et al. 2006). Auxotrophy markers such as *URA3* (uracil), *HIS3* (histidine), or *LEU2* (leucine) are classically used as selection markers, either for maintaining episomal plasmids or for selecting yeasts with modified genomic DNA (Brachmann et al. 1998). Markers conferring resistance to a toxic molecule like geneticin (G418) or hygromycin B may be used too (Decottignies et al. 1998).

6.2.1 Lipids

One general concern with heterologous expression of MPs is the lipid composition of the membrane they are embedded in: interaction of specific lipids has been shown to play an important role in the function of these MPs (Lee and East 1998; Powl et al. 2008; Kapri-Pardes et al. 2011; Whorton and MacKinnon 2011; Haviv et al. 2013). Most of the glycerophospholipids and their derivatives are present in *S. cerevisiae,* although not in identical proportion as in mammalian cells (Blagovic et al. 2001; Blagovic et al. 2005; van Meer et al. 2008; Canadi Juresic and Blagovic 2011).

One of the striking differences between mammalian cells and *S. cerevisiae* is the presence of ergosterol in yeast, a cholesterol analog. For expression of MPs of higher eukaryotes, this may be a disadvantage because the function of several MPs is known to be affected by the nature of the sterol in the membrane phase. For instance, Lagane et al. (2000) demonstrated that ergosterol and cholesterol have opposite effects with respect to the ligand-binding function of a recombinant μ-opioid receptor. However, only a few such examples were reported and some yeast strains have been now engineered to be able to synthesize cholesterol instead of ergosterol (Kitson et al. 2011). Another significant difference resides in the amount of phosphatidylserine (PS) found in the plasma membrane. PS is a minor lipid in most *S. cerevisiae* membranes, except in plasma membrane where it accounts for as much as 30% of the total phospholipids, a higher proportion than that in plasma membranes of mammalian cells (van Meer et al. 2008).

It is important to note that lipid metabolism in yeast is highly variable, depending on the strain used and on culture conditions (Daum et al. 1999). In some cases, overexpression of MPs has also been reported to stimulate membrane biosynthesis and activate quality control mechanisms like unfolded protein response (UPR) and endoplasmic reticulum-associated degradation (ERAD). Such activation suggests that MP trafficking through the secretory pathway may become overwhelmed, leading to accumulation of misfolded neosynthesized MPs and activation of degradation pathways (Griffith et al. 2003; Meusser et al. 2005). For example, Griffith and coworkers showed that an increase in the UPR response is correlated with a dramatic decrease in specific activity of a recombinant P2 adenosine-proton transporter (Griffith et al. 2003). This phenotype is not specific to MP overexpression since it has also been described for a soluble protein (Bleve et al. 2011). Hence, for the sake of increasing the amount of functional protein, the use of adjustable yeast expression systems is probably highly desirable.

6.2.2 Glycosylation

As in other eukaryotes, glycosylation in *S. cerevisiae* starts in the endoplasmic reticulum (ER), where a core structure is transferred to nascent polypeptide chains, and continues in the Golgi apparatus, where this core structure is subsequently modified (Helenius and Aebi 2001). While the core structure is highly similar in all eukaryotes, the nature of *N*-glycan structures found in the Golgi may vary significantly. Glycosylation in yeast is implicated in folding, stability, and function of MPs as in other eukaryotes (Celik and Calik 2012). Because baker's yeast lacks Golgi mannosidases, it is characterized by its ability to hypermannosylate proteins (Gemmill and Trimble 1999), resulting in the addition of more than 40 mannose residues per glycosylation sites. When hypermannosylation occurs, glycosylation is heterogeneous and may affect protein function (Celik and Calik 2012). In mammalian cells, when proteins reach the Golgi apparatus, an appropriate mannosidase removes some of the mannose residues which are then replaced by specific carbohydrates. One option for controlling glycosylation is to remove glycosylation sites by site-directed mutagenesis, but this may result in the biosynthesis of an inactive protein. Several approaches have been attempted to substitute *S. cerevisiae* glycosylation pathways for human pathways and recent advances in the expression of glycoproteins with humanized glycan structures in engineered yeast are promising (Wildt and Gerngross 2005; Chiba and Jigami 2007; Chiba and Akeboshi 2009).

6.2.3 Inventory of Crystal Structures Obtained After Expression in S. cerevisiae

In this section, we present an overview of eukaryotic MPs purified from *S. cerevisiae* membranes, used either as a natural source or as a host for overexpression (Table 6.1).

Most of the already crystallized MPs were obtained from natural sources. One famous result was obtained with adenosine triphosphate (ATP) synthase (Stock et al. 1999) from *S. cerevisiae,* an enzyme responsible for ATP synthesis and which is very abundant in mitochondria. In this case, it was not necessary for researchers to design a particular expression system: they simply purified the protein from a block of baker's yeast conventionally used for cooking. Here, the challenge was to purify and crystallize a large MP complex, as ATP synthase is composed of 17 subunits for the complete assembly of the membrane part (F_0), the catalytic part (F_1), and the peripheral stalk (the latter being lost during purification and crystallization procedures). More recently, the *S. cerevisiae* strain was modified to integrate a hexahistidine tag at the N-terminus of four different mutants of the β subunit (Mueller et al. 2004), leading to the crystallization of the F1 ATPase sub-domain alone (Arsenieva et al. 2010). Crystallization of the whole complex with its F_0 membranous part is in progress (Pagadala et al. 2011).

After heterologous overexpression in *S. cerevisiae,* structures have been obtained for rat and human monoamine oxidase A (rMAOA and hMAOA). The structure of a close isoform, hMAOB, had been previously resolved but after truncation of the C-terminal domain (Binda et al. 2002). Ma and colleagues succeeded in resolving the structure of the whole protein and revealed that the C-terminal 29 residues fold as a helix responsible for anchoring the protein to the mitochondrial outer membrane (Ma and Ito 2002; Ma et al. 2004a, b; Son et al. 2008). Here, yeast cells were transformed with an episomal plasmid carrying the MAOA gene under the control of a galactose-inducible promoter. A classical purification step on a nickel affinity-chromatography resin allowed the authors to obtain about 10 mg of active protein per liter of culture. In this case, particular care was taken with respect to the choice of the detergent for protein solubilization, stabilization, and crystallization: FC-12 proved to be the most efficient detergent for solubilization and stabilization whereas high-resolution diffracting crystals were obtained in the presence of dimethyldecylphosphine. The rMAOA structure represented the first structure of a eukaryotic monotopic MP. Rat and human recombinant enzymes were shown to be isomorphous and displayed close kinetic parameters (Son et al. 2008).

The structure of a plant vacuolar proton-translocating pyrophosphatase was also recently obtained after expression in *S. cerevisiae* (Lin et al. 2012). Expression was performed using a galactose-inducible promoter. The authors chose to overexpress the protein fused to a hexahistidine tag for purification purposes. Note that the same strategy for expression and purification was then used successfully for determining the high-resolution structure of two other PPases from *Thermotoga maritima* (Kellosalo et al. 2012a, b), suggesting that this system is particularly efficient for expressing this class of proteins, regardless of the evolutionary distance between them.

Even more recently, Pryor and coworkers resolved the structure of the Ste24p CAAX protease from *S. mikatae,* which is involved in the maturation of the mating pheromone "a-factor" in yeast (Pryor et al. 2013). The gene encoding Ste24p was cloned downstream of an *ADH2* promoter, a strong constitutive promoter subjected to a tight catabolite repression: its transcription level is repressed several 100-fold in the presence of glucose. In the alternative classical *GAL1–GAL10*-inducible system, glucose is also a strong repressor of transcription, but in that case, after reaching the stationary phase, galactose must be added to the medium to activate transcription of downstream genes. But it is difficult to know exactly when glucose has been completely consumed and in fact, only traces of remaining glucose are sufficient to repress the *GAL1–GAL10* promoter, even in the presence of large amounts of galactose. The use of a constitutive *ADH2* promoter allows to overcome this problem, because expression will start automatically when the glucose concentration is sufficiently low, without any requirement for addition of an extra compound in the medium (Lee and DaSilva 2005). Screening of nine different orthologs of Ste24p identified the one from *S. mikatae* as the most stable and suitable for crystallization trials. For purification of Ste24p, the authors fused an immunoglobulin G (IgG)-binding domain to the C-terminus of Ste24p, as IgG resins have proven to be highly specific compared to Ni^{2+}-chelating resins (Waugh 2005).

The above inventory of those crystal structures of integral eukaryotic MPs which have been obtained after expression in *S. cerevisiae* is rather short, and it is therefore not possible to define a general path leading to success. But this is not specific to overexpression in *S. cerevisiae,* since no general rule emerged either from other expression systems (Bill et al. 2011). Another trail could be to investigate new screening strategies. For example, Li and coworkers developed a medium-throughput pipeline to test homologous expression, solubilization, and purification of 384 MPs from *S. cerevisiae* (Li et al. 2009). This system was subsequently adapted to heterologous expression of MPs from higher eukaryotes (Li et al. 2009). A key feature of this approach is to identify MPs for downstream structural studies on the basis of their size-exclusion profiles, which may reflect protein stability, a critical parameter for crystallization trials. The first step consists in selecting targets on the basis of their primary sequence and their putative number of transmembrane helices, in order to focus on integral transmembrane proteins. The corresponding genes are then cloned under the control of a galactose-inducible *GAL1* promoter, with N-terminal FLAG and C-terminal decahistidine tags. As MP overexpression sometimes turns out to be toxic, some targets are already eliminated after expression trials (Osterberg et al. 2006). For cell lysis, the authors chose to use glass beads in a bead-beater, and for solubilization tests dodecylmaltoside (DDM) was preferred, as this detergent previously proved to be stabilizing for several MPs (Prive 2007). On the 384 targets that Li and coworkers tested, 6 were pushed into the intensive production phase and were readily purified and stable (Li et al. 2009). So far, this strategy resulted in the publication of high-resolution structures for the fungal phosphate/H^+ symporter PiPT (Pedersen et al. 2013) and for the Ca^{2+}/H^+ antiporter Vcx1p from *S. cerevisiae* (Waight et al. 2013).

For decades, our laboratory has been interested in unraveling the relationships between structure and function in the sarco(endo)plasmic reticulum Ca^{2+}-ATPase (Serca1a) Ca^{2+} pump. Among different approaches, we started developing a heterologous expression system of this integral membrane transporter. The subsequent section focuses on the strategy for heterologous overexpression in *S. cerevisiae* our laboratory developed for the Serca1a Ca^{2+} pump, and which led in 2005 to a high-resolution structure.

6.3 Expression in *S. cerevisiae* and Purification of Sarcoplasmic Reticulum (SR) Ca^{2+}-ATPase Serca1a

6.3.1 Structure and Transport Cycle of the SR Ca^{2+}-ATPase Serca1a

Serca1a belongs to the P-type ATPase family of membrane pumps, and plays a critical role in muscle relaxation and Ca^{2+} homeostasis, by transporting Ca^{2+} uphill from the cytosol into the SR lumen (Hasselbach and Makinose 1961; Ebashi and

Lipmann 1962). The P-type ATPase family (organized in five subfamilies called P1, P2, P3, P4, and P5, with the P2 subfamily including for instance the Na^+, K^+- and H^+, K^+-ATPases present in animal cells) is an evolutionarily conserved large family of proteins which is characterized by the formation of an obligatory aspartyl-phosphate intermediate during the pump cycle (Degani and Boyer 1973). P-type ATPases are chemi-osmotic pumps that convert the chemical energy of this aspartyl-phosphate intermediate into active transport of ions.

Probably because of its natural abundance in skeletal muscle, the SR Ca^{2+}-ATPase was the first P-type ATPase for which the three-dimensional (3D) structure was solved (Toyoshima et al. 2000; Toyoshima and Nomura 2002). Since then, X-ray structures of analogs of the most relevant intermediate states in the Ca^{2+}-ATPase transport cycle have been obtained (some of which are shown in Fig. 6.1), providing insights into the molecular events leading to Ca^{2+} translocation across the ER/SR membrane (e.g., Toyoshima et al. 2000, 2007; Toyoshima and Nomura 2002; Sorensen et al. 2004; Olesen et al. 2007). These high-resolution structures confirmed most of the previous suggestions based on site-directed mutagenesis (Andersen 1995), spectroscopic studies (Bigelow and Inesi 1992), or low-resolution structures (Dux and Martonosi 1983; Toyoshima et al. 1993; Zhang et al. 1998). In these structures, the cytosolic portion of the pump is made of three distinct domains: the nucleotide-binding (N) domain, the phosphorylation (P) domain, and the actuator (A) domain (Fig. 6.1). The N domain binds the nucleotide and positions the γ-phosphoryl of ATP for a nucleophilic attack on the conserved aspartate residue located in the P domain, while the A domain contains a strongly conserved TGES motif involved in the dephosphorylation of the aspartate. These cytosolic domains are connected to a transmembrane (M) domain consisting of 10 α-helices (for Serca1a), *via* a linker region which is crucial for transmitting events from the cytosolic catalytic portion of the pump to the cation-binding sites where transmembrane transport does actually occur.

The transport cycle of P-type ATPases from the P2 subfamily (cation transporters) has been worked out in detail. Briefly, and as depicted in Fig. 6.1, it starts with binding of the ions(s) to be transported (two Ca^{2+} ions in the case of Serca1a) to a conformation called "E1," which has high-affinity binding sites for Ca^{2+} within the membrane domain, and accessible from the cytosolic side. Binding of the ion(s) allows the aspartic acid to become phosphorylated from Mg^{2+}-ATP. The resulting high-energy "$Ca_2E1 \sim P$" intermediate is then converted to an "E2P" intermediate, this step being accompanied by the release of the ion to the exoplasmic side. The transport site now has high affinity for a counter-transported ion species (two to three protons per ATP hydrolytic cycle in the case of Serca1a). Hydrolysis of the phosphorylated aspartic acid drives the enzyme back to the "E2" conformation.

Shortly after cloning the *SERCA1a* gene (Brandl et al. 1986), various host cell systems (for example COS cells or insect cells) have been developed for heterologous expression of Serca1a, in order to dissect by site-directed mutagenesis the molecular mechanism for Ca^{2+} transport (Maruyama and MacLennan 1988; Zhang et al. 2000; Miras et al. 2001). These systems have been very successful for

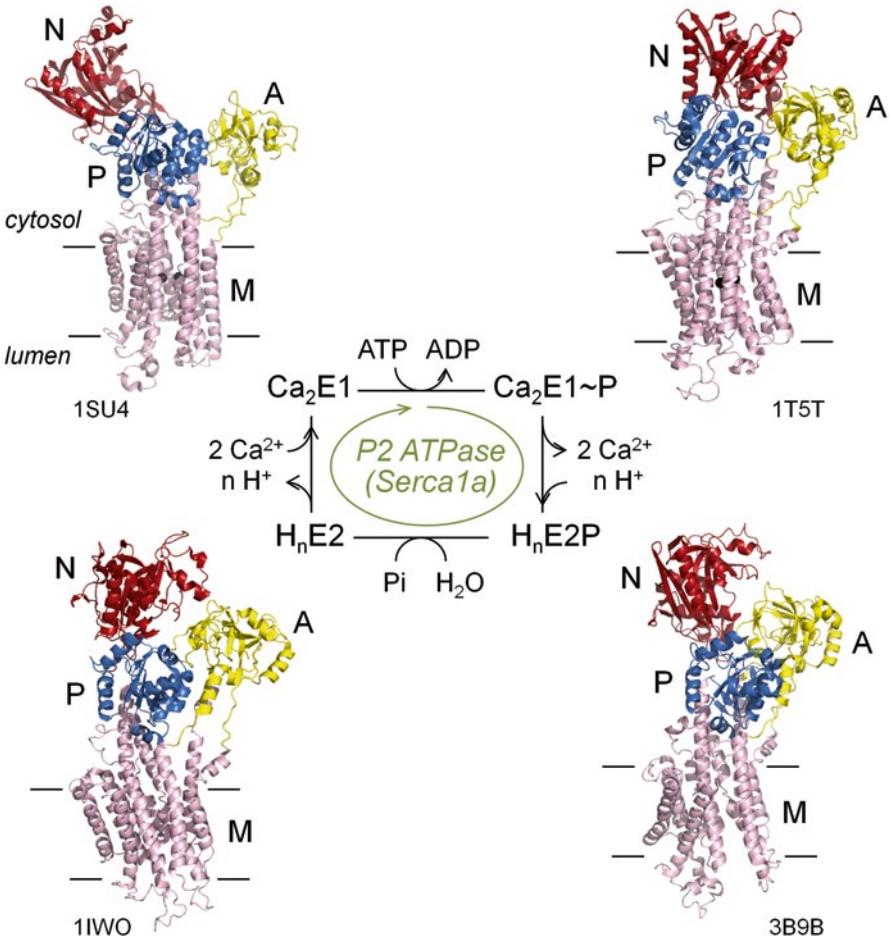

Fig. 6.1 Key intermediates in the catalytic cycle of Serca1a and 3D structures of their analogs. The cycle starts with the exchange of n protons with two Ca^{2+} ions in the cytosol. The Ca^{2+}-bound ATPase is then phosphorylated from ATP to give the $Ca_2E1\sim P$ state, which is converted to the *E2P* state after exchange of two Ca^{2+} ions with n protons. Hydrolysis of the phosphorylated aspartic acid drives the enzyme back to the *E2* conformation. The structures are shown as cartoons, with the *N* domain in *red,* the *P* domain in *blue,* the *A* domain in *yellow,* and the *M* domain in *light pink.* Ca^{2+} ions are shown as *black spheres.* The approximate boundaries of the membrane bilayer are indicated by *solid horizontal lines.* Protein Data Bank (PDB) accession codes: 1SU4 (Ca_2E1 form, obtained in the presence of Ca^{2+}); 1T5T ($Ca_2E1\sim P$ form; obtained in the presence of Ca^{2+}, Mg^{2+}, K^+, ADP, and AlF_4^-); 3B9B (*E2P* form, obtained in the presence of Mg^{2+} and BeF_3^-); 1IWO (*E2* form, obtained in the presence of Thapsigargin, a specific inhibitor of SERCAs)

identification of residues or regions of the protein critical for transport and catalysis (Clarke et al. 1989; Andersen and Vilsen 1992; Strock et al. 1998). However, in spite of high expression levels, these cells are generally grown in too small quantities to allow purification at a reasonable cost of amounts compatible with crystallization trials.

6.3.2 Optimization of Serca1a Expression in S. cerevisiae

In this context, rabbit Serca1a heterologous expression in our laboratory began in the early 1990s, by using the yeast *S. cerevisiae* (Centeno et al. 1994). The initial strategy consisted in inserting the *SERCA1a* complementary DNA (cDNA) in a high-copy-number plasmid, pYeDP1/8–10 (Pompon 1988), under the control of an inducible promoter, with the rationale that delaying the expression phase until the end of the growth phase should allow to overcome potential toxicity problems associated with overexpression of a foreign protein. In pYeDP1/8–10, the strong *GAL10–CYC1* hybrid promoter is fully repressed by glucose present in the medium and when glucose is exhausted (corresponding here to the end of the exponential phase, as deduced from glucose titration assays), addition of galactose triggers induction of the target gene. The *GAL10–CYC1* hybrid promoter contains a sequence called the *GAL* upstream activating sequence (UAS_G) which is required for the induction of the *GAL10* gene in the presence of the product of the *GAL4* regulatory gene (Guarente et al. 1982; West et al. 1984). In addition, this hybrid promoter contains functional TATA elements of the *CYC1* gene that are DNA regions essential for transcriptional initiation by RNA polymerase II (Li and Sherman 1991), as well as the transcription initiation region of the *CYC1* gene itself (Guarente et al. 1982).

Using this expression system, the heterologously expressed Ca^{2+}-ATPase was recovered in the plasma membrane fraction (and to a lesser extent in the microsomes), yielding ~0.3 % of total proteins in the plasma membrane (Centeno et al. 1994). Despite this rather low expression level, the total amount produced was quite substantial since about 1 mg Ca^{2+}-ATPase could be obtained per liter of culture. In addition, the expressed Ca^{2+} pump was functional, as judged by its ability to form a phosphoenzyme form [γ–^{32}P]ATP and by the fact that its specific ATP hydrolysis activity was similar to that of native SR Ca^{2+}-ATPase (Centeno et al. 1994).

A significant step forward was then made by optimizing the expression plasmid as well as the host strain.

Optimization of the expression plasmid was achieved by using the pYeDP60 plasmid designed by Pompon and colleagues (Pompon et al. 1996), a plasmid identical to the pYeDP1/8–10 plasmid except for the presence of an additional selection marker, *ADE2* (Fig. 6.2a). This selection marker is of special interest since even rich culture media become rapidly deprived of adenine upon yeast growth at high cell densities. Thus, in contrast to yeast cells transformed with pYeDP1/8–10, yeast cells auxotroph for adenine and transformed with pYeDP60 could grow in rich medium (where the cell density can rise up to a level about fivefold to tenfold higher than in minimal medium) with minimal plasmid loss. Adding the *ADE2* selection marker turned out to be critical as, thanks to the increased maximal cell density, the expression level reached ~8 mg Ca^{2+}-ATPase per liter of rich culture medium (compared with ~1.5 mg Ca^{2+}-ATPase per liter of minimal medium, as shown in Fig. 6.2b; Lenoir et al. 2002). This corresponded to production of Serca1a up to about 0.7 % of yeast total proteins (not shown), or even 1 % of yeast total proteins after performing two successive galactose inductions (open circles in Fig. 6.2c).

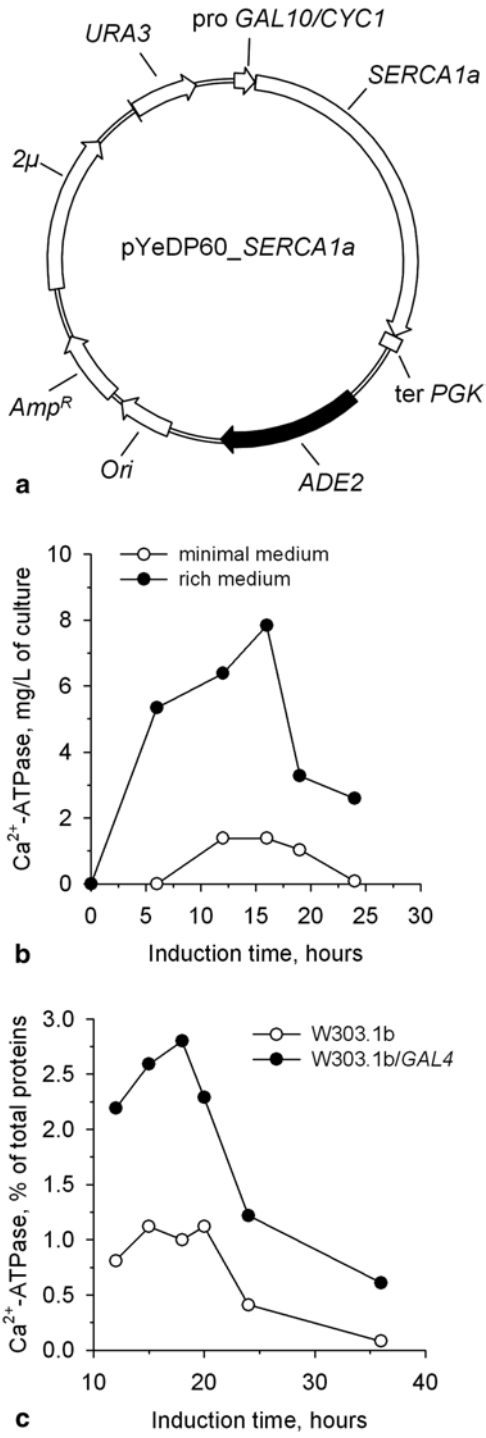

Fig. 6.2 Optimization of Serca1a expression. **a** Map of the pYeDP60 plasmid used for the expression of *SERCA1a*. *ADE2* auxotrophy selection marker for adenine, represented as a *black arrow* for emphasis; *Ori* bacterial replication origin; Amp^R gene conferring resistance to ampicillin; *2μ* yeast replication origin; *URA3* auxotrophy selection marker for uracil; *pro GAL10/CYC1* strong hybrid galactose-inducible promoter; *ter PGK* sequence of the phosphoglycerate kinase used for termination of transcription. **b** Comparison of *Serca1a* expression from yeast growing in rich (●) or minimal (○) medium. The W303.1b yeast strain was grown at 28 °C in either rich or minimal medium. At time zero, expression was triggered by addition of 2% galactose. **c** Optimization of the host strain. An additional copy of the *GAL4* gene was inserted at the Trp locus of W303.1b yeast strain, resulting in the W303.1b/*GAL4* strain. W303.1b (○) and W303.1b/*GAL4* (●) yeast strains were transformed with pYeDP60 and grown in rich medium. Two galactose inductions (2% w/v each time) were performed here; a first one at time zero and a second one 13 h later. Panels **b** and **c** adapted from Lenoir et al. (2002)

Further improvement of Ca^{2+}-ATPase expression was achieved by manipulating the W303.1b host strain. A common limitation to the use of recombinant *GAL* promoters for the controlled high-level expression of foreign proteins is the inherent low expression level of the *GAL4* gene product, Gal4p, which mediates expression of proteins that are under the control of *GAL* promoters (Romanos et al. 1992). To overcome this limitation, we integrated a hybrid gene in the yeast chromosome, consisting of the *GAL10* promoter fused to the *GAL4* gene (Schultz et al. 1987; Pedersen et al. 1996). In this manner, the expression of Gal4p is increased in the presence of galactose, as well as that of the foreign protein. This is especially helpful for expression of proteins from multi-copy plasmids (2μ-based plasmids). The resulting yeast strain, W303.1b/*GAL4* was compared with the W303.1b parental strain for its ability to overexpress Serca1a. As illustrated by the black circles in Fig. 6.2c, the expression level of Serca1a reached a maximum of almost 3 % of total yeast proteins, thus about ten times more than that reported by Centeno and colleagues (Centeno et al. 1994), and 30 mg Ca^{2+}-ATPase could be recovered for 1 L of culture (Lenoir et al. 2002).

Another critical parameter was the control of temperature during the expression phase. As already observed in bacteria and other yeast expression systems, decreasing the temperature from 28 to 18 °C significantly increased the amount of properly folded and active protein (Lenoir et al. 2002). One obvious reason for this is that the yeast metabolism is slowed down, thereby facilitating integration by the translocon of newly synthesized proteins into the ER membrane. When after yeast breakage differential centrifugation was performed to roughly separate a "heavy" membrane fraction (sedimenting at rather low-speed centrifugation, ~20,000 g), from a "light" membrane fraction (recovered after high-speed centrifugation, ~100,000 g), we observed that the temperature influenced the final destination of the expressed Serca1a toward the "light" membrane fraction. The "heavy" fraction is poorly solubilized by mild detergents, with the solubilized fraction containing low amounts of active Serca1a, while the "light" membrane fraction is more easily solubilized and contains higher amounts of active protein. In sum, although shifting temperature to 18 °C during the expression phase decreases Serca1a overexpression, the quality of the protein expressed at 18 °C is enhanced (Lenoir et al. 2002). In the "light" fraction, recombinant Serca1a finally accounts for ~1.5–2 % of total MPs (~6–8 mg Serca1a per liter of culture).

6.3.3 Affinity Purification of Serca1a

Initial *SERCA1a* constructs were cloned in frame with a C-terminal hexahistidine tag, for subsequent affinity purification by immobilized metal ion affinity chromatography. The yield of this purification step was about 20 %, allowing the recovery of about 1 mg Ca^{2+}-ATPase from 1 L of yeast culture, and with a purity estimated to be about 50 %. Although this proved to be sufficient for functional studies of wild-type and mutated Ca^{2+}-ATPases (Lenoir et al. 2004, 2006), the relatively low purity

of the sample was not compatible with crystallization trials. Toward this goal, we resorted to the extraordinarily high affinity of avidin for biotin.

Biotin (vitamin H) is a small coenzyme synthesized by plants, most bacteria, and some fungi, which is bound to a specific lysine at the active site of biotinylated proteins *via* an amide linkage. The biotinylation reaction is performed by biotin protein ligases (Chapman-Smith and Cronan 1999). The biotinylation reaction catalyzed by biotin protein ligases is very specific, and there are only a scarce number of biotinylated proteins (only one in *E. coli* and up to five in most other organisms). Biotinylated proteins are multi-subunit enzymes that play roles in metabolic carboxylation/decarboxylation and transcarboxylation reactions, such as the oxaloacetate decarboxylation reaction. The biotinylation domain is strongly conserved among biotinylated proteins (Schwarz et al. 1988). This region is usually located at the C-terminus of the polypeptide chain and the lysine residue that becomes modified with biotin is generally located 34 or 35 residues upstream from the C-terminus (Chapman-Smith and Cronan 1999).

Using various biotinylated proteins, it has been shown that the minimum size of the segment required for biotinylation is 75 amino acids long, starting from the protein C-terminus. This sequence, when added to the C-terminus of β-galactosidase, is indeed sufficient to promote biotinylation of the fusion protein expressed in *E. coli* (Cronan 1990). Importantly, that study also showed that a bacterial biotin-acceptor sequence also functions in yeast, paving the way for expression of proteins fused to biotin-acceptor domain (BAD) in eukaryotic expression systems (Cronan 1990).

The specific and high affinity between tetrameric streptavidin and biotin (Kd $\sim 10^{-14}$ mol/L) can be used to purify biotinylated proteins. Such strategy has been successfully used for the purification in a single step of various proteins, including MPs such as lactose permease expressed in *E. coli* (Consler et al. 1993; Pouny et al. 1998), a plant sucrose carrier (Stolz et al. 1995) and human P-glycoprotein (Howard and Roepe 2003), both expressed in *S. cerevisiae*. However, because of the extremely tight binding between tetrameric streptavidin and biotin, harsh conditions are required to disrupt their interaction, often leading to denaturation of the protein of interest.

We therefore used an alternative procedure for purification purposes. We fused the last 93 residues of the BAD of the α-subunit of oxaloacetate decarboxylase, a biotinylated enzyme from *Klebsiella pneumoniae,* to the C-terminus of Serca1a, but to circumvent problems associated with the subsequent release of the fusion protein from avidin beads (even using monomeric avidin, which has a reduced affinity for biotin), a thrombin cleavage site was inserted between Serca1a and BAD (Fig. 6.3a; Jidenko et al. 2006). The recombinant Serca1a-BAD was then expressed using the above-described pYeDP60 plasmid, in the *S. cerevisiae* strain W303.1b/*GAL4*. Serca1a-BAD proved to experience biotinylation in vivo, and after solubilization of yeast membranes with n-dodecyl β-D-maltoside (DDM), the biotinylated protein was retained specifically onto monomeric avidin-coupled resin (Fig. 6.3b, lane "R_0"; Jidenko et al. 2006). Note that naturally occurring yeast biotinylated proteins were also retained onto avidin beads, but the treatment of the resin with thrombin (lane "R_{60}") allowed to specifically elute Serca1a (lane "E"), without its BAD

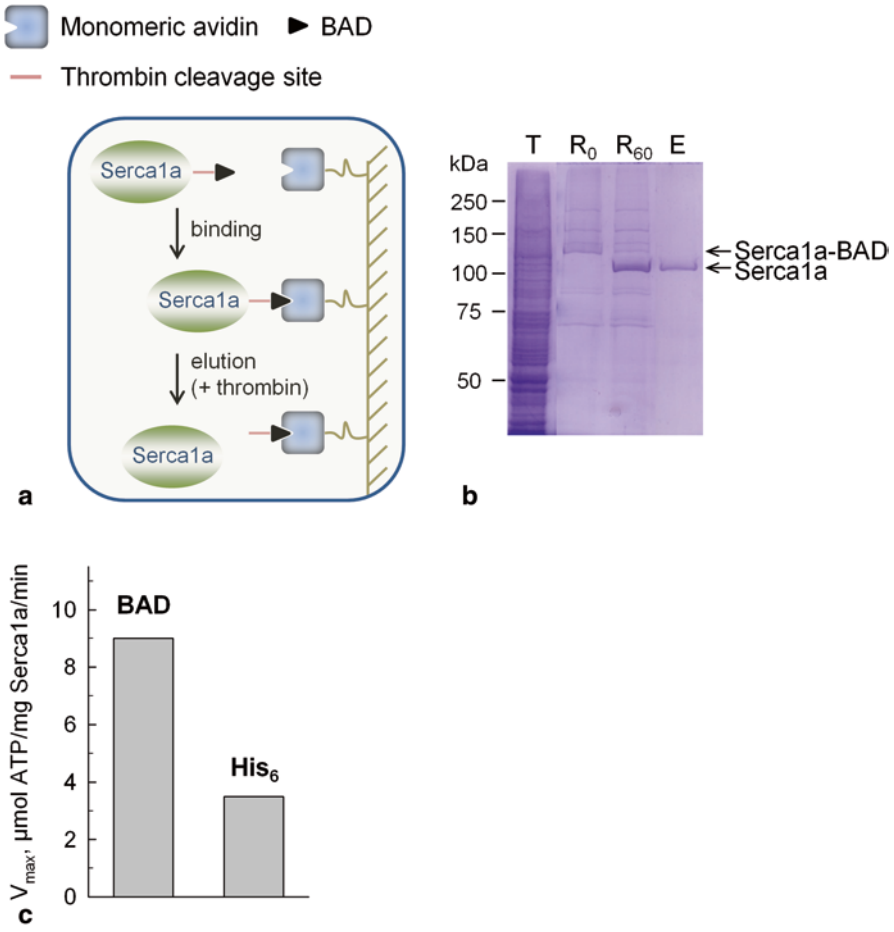

Fig. 6.3 Affinity purification of *Serca1a* in a functional form. **a** Purification scheme. The C-terminally *BAD*-tagged *Serca1a* (Serca1a-BAD) is solubilized from yeast membranes with DDM and applied onto a *monomeric avidin* resin. A *thrombin cleavage site* located between *Serca1a* and the *BAD* tag allows elution of *Serca1a* from the resin. **b** SDS-PAGE analysis of *Serca1a* purification. *T* total—starting yeast membrane fraction, expressing *Serca1a-BAD*; R_0 resin—aliquot of the monomeric avidin resin before treatment with thrombin, showing proteins bound to the resin; R_{60} aliquot of the avidin resin after a 60-min incubation with thrombin; *E* eluate fraction recovered after thrombin cleavage. Proteins were run onto an 8 % Laemmli-type acrylamide gel and stained with Coomassie blue. **c** Maximum velocity of Ca^{2+}-dependent ATP hydrolysis by Serca1a purified either from an initial *BAD*-tagged construct or from a *His*-tagged construct. ATPase activity was assayed spectrophotometrically at 30 °C. (Adapted from Jidenko et al. 2006)

moiety. At this stage, Serca1a was in a relatively pure form (Fig. 6.3b) and the yield of purification was estimated to be about 6 %. As much as 0.3 mg Serca1a was recovered from 1 L yeast culture. Beyond the fact that purification on monomeric avidin yielded a more homogeneous sample than affinity purification on Ni^{2+}-NTA

beads, the purified (initially BAD-tagged) enzyme displayed a maximal rate of ATP hydrolysis of about 9 µmol/mg Serca1a/min at 30 °C, about twofold to threefold higher than that of the His-tagged enzyme (Fig. 6.3c), suggesting either that the six histidines located at the C-terminus of Serca1a are deleterious for enzyme activity (as the His_6 tag was not removed after purification) or that active ATPases are somehow preferentially selected by the avidin purification procedure (Jidenko et al. 2006). The latter hypothesis is consistent with the idea that only correctly folded biotinylation domains will be biotinylated, ensuring that misfolded biotinylation domains will not be purified, whereas using histidine tags will not make it possible to sort correctly folded from misfolded fusion proteins.

6.3.4 Crystallization and Structure Determination of Heterologously Expressed Wild-Type and Mutated Serca1a

This system has been the cornerstone for purification of Serca1a, after its heterologous expression in yeast. However, a major improvement for subsequent structural characterization came from the introduction of a second purification step, namely size-exclusion chromatography (SEC-HPLC). Such extra purification step made it possible to eliminate the small amounts of aggregates and contaminants (including the thrombin protease), to increase the purity of the sample, and, most importantly, to simultaneously allow for detergent exchange (Jidenko et al. 2005). Indeed, the type of detergent chosen for crystallization attempts is a critical parameter, because it will influence both the stability of the protein and its capability to form crystals (Sorensen et al. 2006). As octaethylene glycol mono-*n*-dodecyl ether ($C_{12}E_8$) had previously proven superior to DDM for crystallogenesis of several P-type ATPases (Toyoshima et al. 2000; Sorensen et al. 2004), DDM was exchanged for $C_{12}E_8$ during the above-mentioned SEC-HPLC step (Jidenko et al. 2005).

After concentration of the purified sample to ~10 mg/mL and relipidation with 1,2-dioleoyl-sn-glycero-3-phosphocholine (DOPC), crystallization conditions were explored using a screen based on conditions identified with native Serca1a (Sorensen et al. 2004). Crystals obtained in the presence of AMPPCP, a nonhydrolyzable ATP analog, and Ca^{2+}, diffracted beyond 3.1 Å, and the diffraction properties were similar to those of native Serca1a, without any significant structural difference between the recombinant Serca1a (Fig. 6.4a) and its native counterpart crystallized under the same conditions. Binding of AMPPCP takes place at a highly conserved region located at the interface between N and P domains (inset of Fig. 6.4a) and AMPPCP can be found in very close proximity to the invariant phosphorylated aspartate found in all P-type ATPases (D351 in the case of Serca1a). The two Ca^{2+} ions that are transported at the expense of one ATP molecule per ATPase cycle are coordinated by residues located in the membrane domain (M; inset of Fig. 6.4a). This structure, together with that of a mammalian voltage-dependent K^+ channel, represent the first two crystal structures for mammalian integral transmembrane proteins produced in a heterologous system (Jidenko et al. 2005; Long et al. 2005; Midgett and Madden 2007).

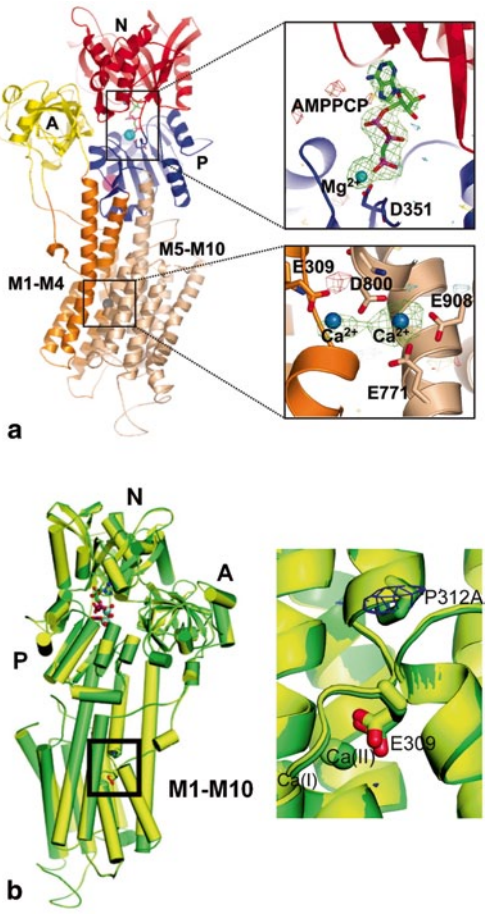

Fig. 6.4 X-ray 3D structures of recombinant Serca1a expressed in yeast. **a** Structure of recombinant rabbit wild-type Serca1a. The structure, obtained in the presence of Ca^{2+} and AMP-PCP, is shown as cartoon with the *N* domain displayed in *red,* the *P* domain in *blue,* the *A* domain in *yellow,* the first four TM helices in *orange,* and the last six TM helices in *light pink.* Two critical regions involved in nucleotide binding and autophosphorylation, and in Ca^{2+} binding, are magnified. Reproduced from Jidenko et al. (2005). **b** Structure of recombinant rabbit *P312A* mutant of Serca1a. The structure was obtained in the presence of ADP and the phosphate analog AlF_4^-. On the *left,* the crystal structure of *P312A* (*yellow*) is superimposed with the wild-type structure in the same conditions (*green*). On the *right,* magnification of the Ca^{2+}-binding site in the transmembrane region underlining the fact that no significant differences are observed between wild-type and *P312A* structures. P312 or A312, and E309 are indicated. (Reproduced from Marchand et al. 2008)

Obtaining the structure of the heterologously expressed wild-type Serca1a has paved the way toward analysis of the structure of mutated proteins. Indeed, many mutations have been reported to interfere with the Ca^{2+}-ATPase catalytic cycle (Andersen 1995), but whether the effect of these mutations reflects a genuine alteration of partial reactions of the catalytic cycle or whether it is the result of a global structural change remained to be determined. Along those lines, the P312A mutation in Serca1a, which had been previously reported as interfering with ATP hydrolysis and Ca^{2+} transport (Vilsen et al. 1989), has been selected. P312 is located in transmembrane segment M4, next to the ^{308}PEGL motif containing the E309 residue involved in Ca^{2+} binding. Studying the partial reactions of P312A catalytic cycle

revealed that the rate of the $Ca_2E1\sim P \rightarrow E2P$ transition was dramatically decreased (Vilsen et al. 1989). The P312A mutant was expressed and purified using our procedure, and subsequently crystallized (Marchand et al. 2008). Crystallization was performed in the presence of AlF_4^- and adenosine diphosphate (ADP) together with 10 mM Ca^{2+} in order to mimic the ADP-sensitive phosphoenzyme $Ca_2E1\sim P$. The crystal structure of the P312A mutant displayed a high degree of isomorphism with that of the wild-type enzyme (Fig. 6.4b), and it was thus concluded that the severe functional consequences of this mutation were associated with only minor structural changes (Marchand et al. 2008). It was proposed in that work that replacing P312 by an alanine does stabilize the $Ca_2E1\sim P$ conformation by facilitating hydrogen bonding between P308 and A312. This mutation would thus relieve an inbuilt constrained region at site I (Marchand et al. 2008).

These achievements with expressed Serca1a were the basis for attempting to overexpress in yeast (and purify) other MPs, as exemplified below by the lipid "flippase" Drs2p/Cdc50p complex.

6.4 Coordinated Overexpression of the Lipid "Flippase" Complex Drs2p/Cdc50p

6.4.1 Transbilayer Phospholipid Asymmetry in Eukaryotic Cell Membranes

Studying how membrane transport proteins termed "flippases" create and maintain phospholipid asymmetry in eukaryotic cell membranes is rapidly expanding, because of the influence of membrane lipid asymmetry on a multitude of cellular functions. Prime candidates for this transport activity are P-type ATPases from the P4 subfamily (hereafter referred to as P4-ATPases), but the mechanism for phospholipid transport by P4-ATPases remains largely elusive (Poulsen et al. 2008b; Coleman et al. 2012).

Let us first recall that eukaryotic cells contain thousands of different lipid structures. This diversity reflects numerous different functions for cellular lipids: in addition to their role in cell compartmentalization, they are used for energy storage, as important regulatory molecules, or they may act as first or second messengers in signal transduction (van Meer et al. 2008). In membranes of the late secretory pathway, this range of functions is accompanied by a particular distribution of lipids: The *trans*-Golgi network (TGN), as well as the plasma and endosomal membranes, display an asymmetric transbilayer distribution with PS and phosphatidylethanolamine (PE) primarily restricted to the cytosolic leaflet, and sphingomyelin (SM) and glycosphingolipids (GSLs) mainly residing in the noncytosolic leaflet (Op den Kamp 1979; Daleke 2007). Such an asymmetric distribution has important functional consequences. For instance, the strong interaction between GSLs and sterols ensures a high stability and impermeability of the plasma membrane; conversely,

the enrichment of aminophospholipids in the cytosolic leaflet of the plasma membrane and on the surface of endocytic and exocytic vesicles may help to keep these membranes in a fusion-competent state (Kinnunen and Holopainen 2000).

6.4.2 P4-ATPases and Cdc50 Proteins as Prime Candidates for Phospholipid Translocation

P4-ATPases are thought to play a prominent role in creating and maintaining this phospholipid asymmetry, by selectively translocating lipids (instead of translocating ions, like members of most P-type ATPase subfamilies), mainly PS and PE, from the luminal leaflet to the cytosolic leaflet of plasma membranes as well as of TGN membranes (Graham 2004; Daleke 2007). This lipid-translocation activity is thought to be dependent on the intimate coupling of P4-ATPases with accessory subunits known as Cdc50 proteins (Poulsen et al. 2008a; Lenoir et al. 2009; Lopez-Marques et al. 2011).

In plasma membranes, loss of lipid asymmetry and the resulting cell-surface exposure of PS triggers recognition of apoptotic cells by macrophages, activation of the blood coagulation cascade, or virus entry (Rosing et al. 1980; Fadok et al. 2000; Mercer and Helenius 2008). But much remains to be discovered about other physiological roles of lipid asymmetry and the relevance for eukaryotic cells to spend energy to maintain such transbilayer asymmetry in other contexts. This is especially true for unicellular organisms like yeast cells, as they certainly do not need to deal with PS exposure for triggering blood clotting signaling. So, what is lipid translocation also made for? An appealing hypothesis has been provided by the observation that the yeast P4-ATPase Drs2p is required for budding of post-Golgi exocytic vesicles (Gall et al. 2002) and for the formation of clathrin-coated vesicles (Chen et al. 1999). The hypothesis is that by expanding one of the leaflets of the bilayer while reducing phospholipid number in the other one, flippases might drive membrane bending and thereby provide a major contribution to vesicle formation and ultimately vesicle-mediated protein transport (Devaux et al. 2008).

Of note, P4-ATPases are associated with several inherited disorders. For instance, one human disease, progressive familial intrahepatic cholestasis (PFIC1, or Byler disease), has been directly correlated with mutations in a gene encoding a P4-ATPase (*ATP8B1*). PFIC1 is an autosomal recessive disorder for which individuals manifest cholestasis in infancy and which progresses toward end-stage liver disease before adulthood (Bull et al. 1998).

Collectively, these data highlight the crucial importance of P4-ATPases in health and disease and underscore the need for structural and mechanistic insights into the molecular mechanism by which P4-ATPases catalyze lipid transport. We therefore aimed at adapting our overexpression system to P4-ATPases. A specific impetus was that although the wealth of P-type ATPase 3D structures has tremendously expanded in the recent years (Morth et al. 2007; Pedersen et al. 2007; Shinoda et al. 2009; Gourdon et al. 2011), P4-ATPases still lag behind.

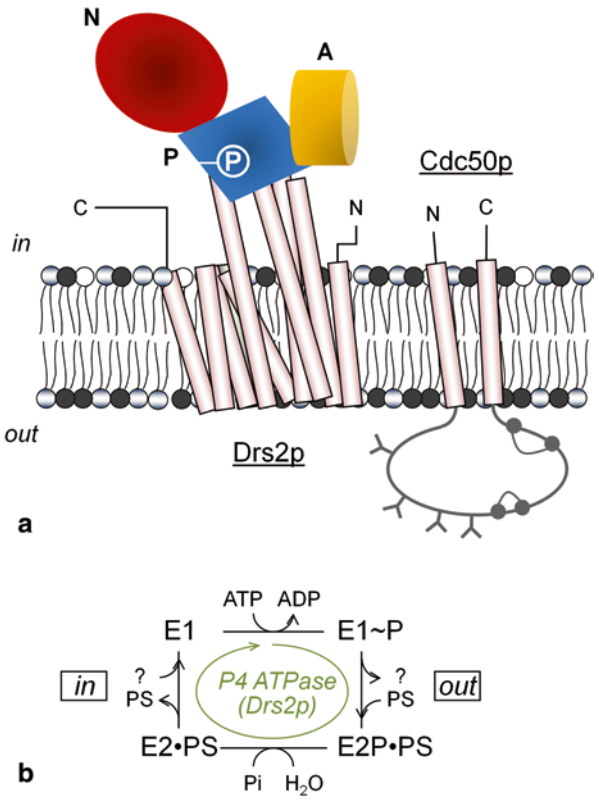

Fig. 6.5 Predicted topology of yeast Drs2p and Cdc50p and putative lipid transport cycle. **a** Predicted topology of Drs2p and Cdc50p. Transmembrane helices of Drs2p and Cdc50p are shown as *light pink cylinders*. The phosphorylation site is indicated in the *P* domain. The phosphorylation domain (*P*) is represented in *blue,* the nucleotide-binding domain (*N*) is represented in *red*, and the actuator (*A*) domain is shown in *yellow.* N- and C-termini are indicated on the cytosolic ("*in*") side of the bilayer. Cysteines of Cdc50p involved in the formation of disulfide bridges and previously identified by site-directed mutagenesis (Puts et al. 2012) are symbolized by *gray dots.* Predicted sites for *N*-glycosylation are also represented on Cdc50p ectodomain. **b** Simplified scheme of the transport cycle for P4-ATPases. Whether phospholipid transport by P4-ATPases (from the outside to the inside) is coupled to transport of another substrate in the opposite direction is currently unknown

There are five P4-ATPase members in yeast: Dnf1p and Dnf2p which reside at the plasma membrane, Drs2p and Dnf3p which reside in the TGN, and Neo1p localized in the endosomes (Gall et al. 2002; Hua et al. 2002). Deletion of Dnf1p and Dnf2p inhibits ATP-dependent transport of fluorescent analogs (nitrobenzoxadiazole (NBD)-labeled) of PC, PS, and PE (Pomorski et al. 2003), while removal of Drs2p and Dnf3p abolishes NBD-PS/PE and NBD-PC/PE transport, respectively (Natarajan et al. 2004; Alder-Baerens et al. 2006). Concerning accessory proteins, genetic disruption of yeast Cdc50 proteins was found to phenocopy *dnf* and *drs2* deletions. This family includes three proteins in yeast, namely Cdc50p, Lem3p, and Crf1p. It is now clear that Cdc50 proteins associate with P4-ATPases and that this association is of primary importance. Indeed, Cdc50 proteins have been shown to be required for stability and export of P4-ATPases from the ER, both in yeast and in mammalian cells (Saito et al. 2004; Chen et al. 2006; Furuta et al. 2007; Paulusma et al. 2008;

van der Velden et al. 2010). Recent evidence also indicates that Cdc50 proteins play an intimate role in the transport cycle catalyzed by P4-ATPases (Poulsen et al. 2008a; Lenoir et al. 2009; Bryde et al. 2010).

Because yeast Drs2p is the one for which the most convincing data suggesting implication in lipid transport have been obtained, we decided to focus on this particular P4-ATPase. Drs2p is predicted to contain ten transmembrane spans and to have an overall domain organization similar (but with long N- and C-terminal extensions) to that of other P–type ATPases from the P2 and P3 subfamilies (Fig. 6.5a). It binds specifically to the Cdc50 protein called Cdc50p. The Cdc50p polypeptide chain is predicted to span the membrane twice, with a large ectodomain protruding toward the TGN lumen (Fig. 6.5a). Two disulfide bridges have been identified in this ectodomain (Puts et al. 2012), the latter also containing four consensus sequences for *N*-linked glycosylation (Fig. 6.5a). As previously discussed, all P-type ATPases, including P4-ATPases, display a clear conservation of the key residues known in P2-ATPases to be involved in ATP binding, transient phosphorylation (the phosphorylated residue is Asp560 in Drs2p), and phosphoenzyme hydrolysis, as well as a common organization of transmembrane helices (Lenoir et al. 2007). Assuming that P2 and P4-ATPases also share similar mechanisms of energy transduction and reaction schemes, PS binding to Drs2p after phosphorylation from ATP, by analogy with proton binding to Serca1a or K^+ binding to Na^+, K^+-ATPase, should stimulate dephosphorylation of the pump, in parallel to its transport to the other leaflet of the bilayer (Fig. 6.5b).

6.4.3 Functional Co(over)Expression of Drs2p and Cdc50p in Yeast Membranes

As most P4-ATPases appear to function as protein complexes, we devised a high-yield co-expression system for the yeast P4-ATPase Drs2p and its accessory subunit Cdc50p.

To facilitate detection of Drs2p and Cdc50p as well as for future purification of the complex, a BAD and a decahistidine tag were added at the C-terminus of Drs2p and Cdc50p, respectively. The fused genes were cloned independently in pYeDP60 expression plasmid, resulting in pYeDP60_*DRS2*-BAD and pYeDP60_*CDC50*-His_{10} (Fig. 6.6). As described for Serca1a in the previous section of this chapter, *DRS2* and *CDC50* genes in this plasmid were both placed under the control of a strong galactose-inducible promoter. From the pYeDP60_*CDC50*-His_{10} vector, a cassette containing the promoter, the *CDC50* coding sequence, and the PGK terminator was then amplified by polymerase chain reaction (PCR) and subsequently inserted in the pYeDP60_*DRS2*-BAD companion plasmid. We thus obtained pYeDP60_*DRS2*-BAD/*CDC50*-His_{10}, appropriate for co-expression of Drs2p-BAD and Cdc50p-His_{10} (Fig. 6.6). The rationale for constructing this co-expression plasmid, rather than expressing the two proteins from different plasmids, was to avoid imbalanced transcription of *DRS2* and *CDC50* genes, because of an unequal number of plasmids in each cell, a frequent behavior of 2μ-based plasmids.

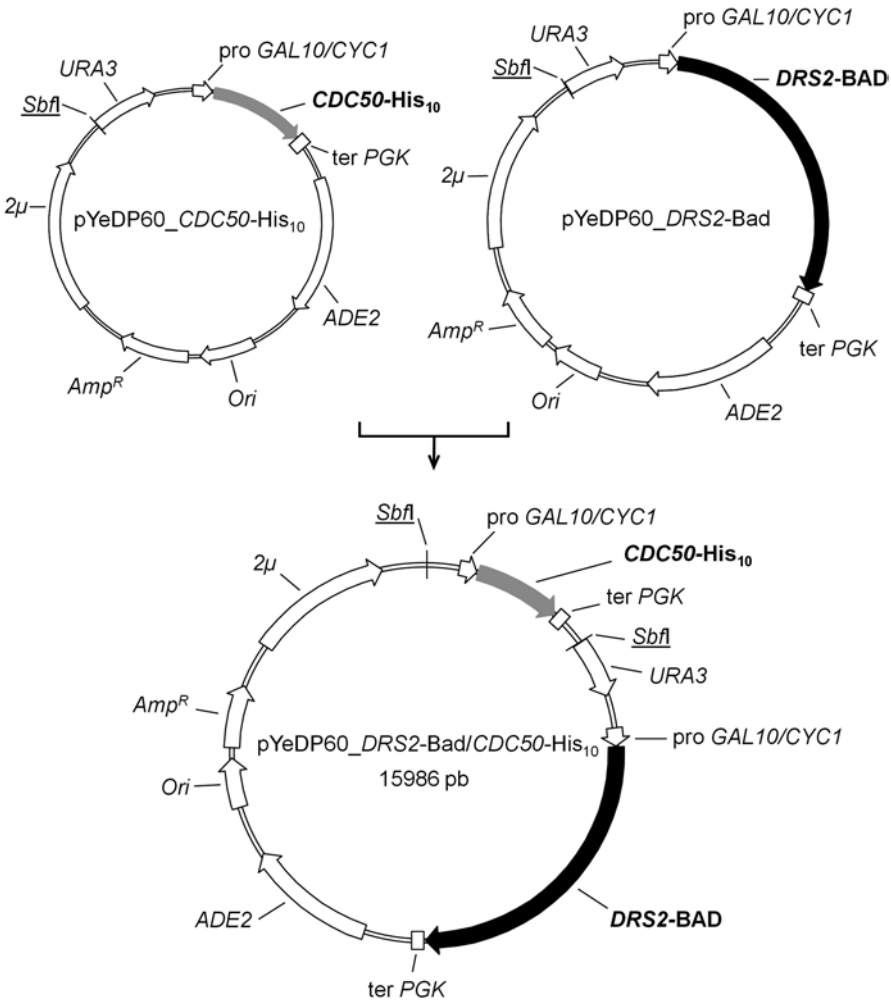

Fig. 6.6 Maps of the plasmids used for co-expression of Drs2p-BAD and Cdc50p-His_{10}. *CDC50* fused to a C-terminal decahistidine tag, His_{10} (*top left, light gray arrow*), and *DRS2* fused to a C-terminal biotin-acceptor domain, BAD (*top right, black arrow*), were first cloned independently in pYeDP60, in both cases under the control of the inducible *GAL10/CYC1* hybrid promoter, using *Eco*RI and *Sma*I restriction sites. This resulted in pYeDP60_*DRS2-BAD* and pYeDP60_*CDC50-His*$_{10}$ plasmids (*top right* and *left,* respectively). A cassette containing the *GAL10/CYC1* promoter, the *CDC50* gene, and the *PGK* terminator was then amplified by PCR from pYeDP60_*CDC50-His*$_{10}$ using primers containing *Sbf*I restriction sites, and inserted in pYeDP60_*DRS2-BAD,* which has a unique *Sbf*I restriction site at position 11 (*underlined*). *ADE2* auxotrophy selection marker for adenine; *Ori* bacterial replication origin; Amp^R gene conferring resistance to ampicillin; *2μ* yeast replication origin; *URA3* auxotrophy selection marker for uracil

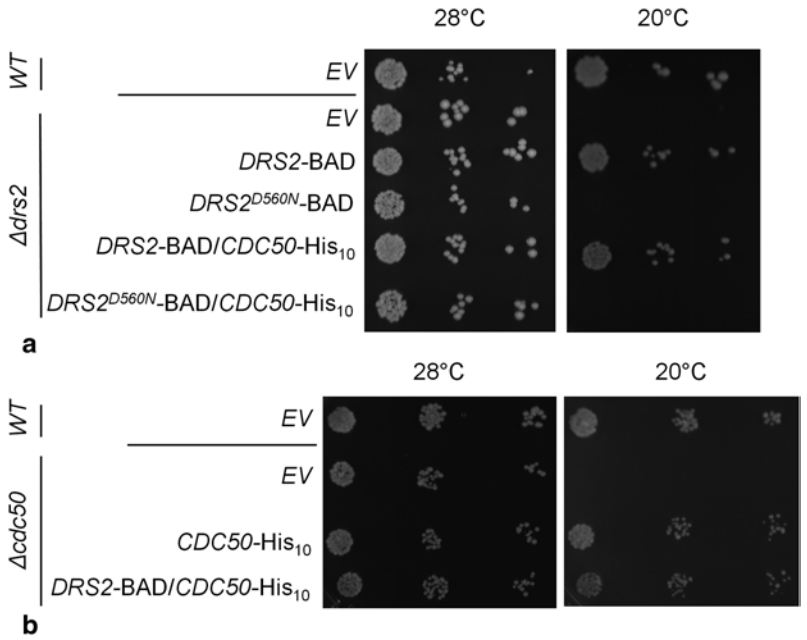

Fig. 6.7 Overexpressed Drs2p and Cdc50p restore the ability of *Δdrs2* and *Δcdc50* yeast cells for growth at low temperatures. Yeast cells, either wild-type W303.1b/*GAL4–2* cells or *Δdrs2* or *Δcdc50* mutants, were transformed with various vectors. Wild-type cells transformed with an empty vector (EV) were used as negative control. The *Δdrs2* mutant was transformed in order to express *DRS2* alone or in combination with *CDC50* (**a**), and the *Δcdc50* mutant was transformed in order to express *CDC50* alone or in combination with *DRS2* (**b**). *DRS2* (wild type or mutated at its catalytic aspartate, $DRS2^{D560N}$) was tagged with a sequence coding for BAD at its C-terminus, and *CDC50* was tagged with a decahistidine tag (His_{10}) at its C-terminus. Serial dilutions of yeast cells were spotted onto a medium containing 2 % galactose (and 2 % fructose) for growth at either 28 °C (left) or at the restrictive temperature of 20 °C (right), for 3–5 days.

We checked the functionality of our constructs by taking advantage of the fact that *Δdrs2* yeast cells exhibit a cold-sensitive growth phenotype (Chen et al. 1999). As can be seen from Fig. 6.7a, BAD-tagged Drs2p restored the ability of *Δdrs2* cells for growth at 20 °C in a galactose-containing medium, whereas a "dead" mutant of Drs2p, for which the catalytic Asp560 residue had been swapped for an Asn, did not, thus confirming that catalytic activity of Drs2p is required for growth at low temperature. Drs2p-BAD, expressed together with Cdc50p-His_{10} thanks to our co-expression plasmid also restored growth of *Δdrs2 at* 20 °C. Similarly, Fig. 6.7b shows that constructs for Cdc50p, tagged with ten histidines at its C-terminus, restored growth of *Δcdc50* cells at 20 °C. The same was true if Cdc50p-His_{10} was expressed from the co-expression plasmid (Fig. 6.7b).

We then turned to large-scale production of Drs2p and Cdc50p. Yeasts transformed with the pYeDP60_*DRS2*-BAD/*CDC50*-His_{10} plasmid were first precultured in minimal medium, at 28 °C (Fig. 6.8a). Yeast cells were then grown in a

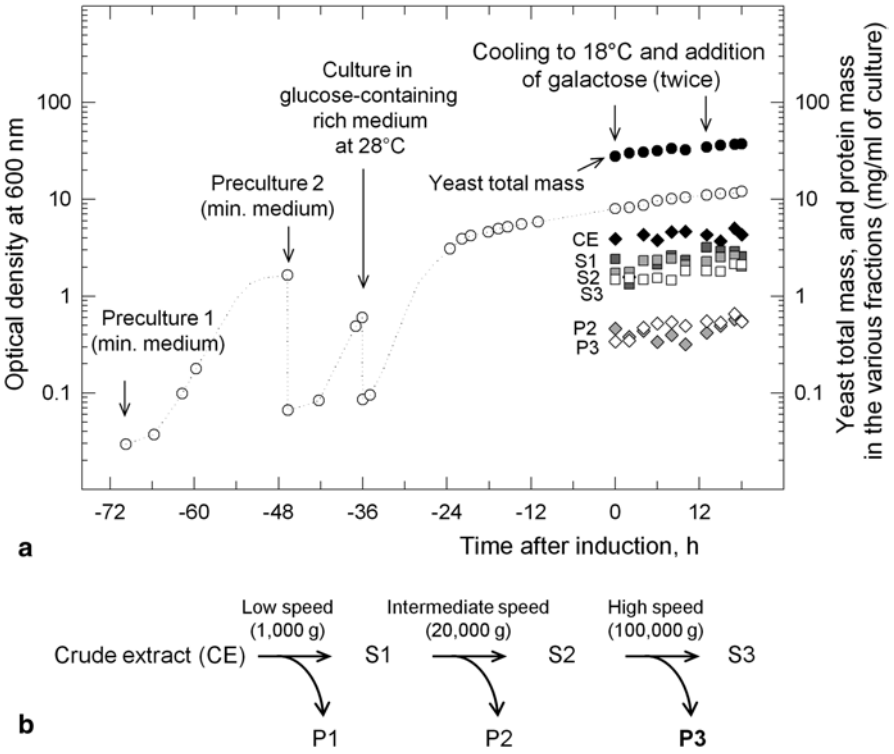

Fig. 6.8 Follow-up of yeast growth and membrane fractionation. **a** Yeast growth and expression phase, as monitored by turbidity measurements (*open circles*). Two precultures in minimal medium were performed (between -70 and -36 h) before yeast growth in rich medium (between -36 h and time zero) and the subsequent induction of expression (between time zero and 18 h). After various times of induction, the protein content of crude extract (*CE*) fractions recovered after yeast breakage with beads is indicated by *black diamonds*. **b** Schematic outline of the membrane fractionation procedure. In panel **a**, the total protein content of the *S1* low-speed supernatant (*dark gray squares*) as well as that of the *S2* (*light gray squares*) and *S3* (*white squares*) supernatants, and of the *P2* (*light gray diamonds*) and *P3* (*white diamonds*) pellets, are also indicated.

(glucose-containing) rich medium for 36 h, until a slower phase was reached, revealing glucose depletion from the medium (Fig. 6.8a). The biomass reached an absorbance at 600 nm of about 10 (using a Novaspec II Pharmacia spectrophotometer) at that stage, corresponding to roughly 30–40 g yeast cells per liter of culture. Expression of Drs2p-BAD and Cdc50p-His_{10} was then induced by adding galactose (time zero in Fig. 6.8a) and simultaneously lowering temperature to 18 °C, to improve protein folding and sorting. After 13 h, a second galactose addition was performed, for 5 more hours. Yeast aliquots were sampled during the expression phase, and after yeast breakage, various fractions were recovered by differential centrifugations, among which membrane pellets recovered at moderate and high

speed, P2 and P3, respectively (Fig. 6.8b). This protocol made it possible to collect about 0.5 g P3 membranes per liter of culture at the end (white diamonds in Fig. 6.8a). The various fractions were analyzed for their contents in Drs2p-BAD and Cdc50p-His_{10}, using a biotin probe and a His probe, respectively. Drs2p-BAD expression (Fig. 6.9a) increased progressively after induction by galactose, to reach a quasi-plateau after 17–18 h in both P3 and P2 membranes. Endogenous yeast biotinylated proteins (among which Pyc1/2p and Arc1p) were detected as faint bands. Cdc50p-His_{10} (Fig. 6.9b) was detected as several bands corresponding to various glycosylation levels, the fastest one corresponding to core unglycosylated Cdc50p-His_{10} (Jacquot et al. 2012) and the others to Cdc50p-His_{10} glycosylated to various degrees.

Remarkably, the pattern of Cdc50p-His_{10} glycosylation exhibited significant differences in P2 membranes *versus* P3 membranes (Fig. 6.9b and c). As a function of time, fair glycosylation of Cdc50p was observed in P2 membranes after a few hours of induction, but the ratio between the mature (glycosylated) and the non-mature forms of Cdc50p was clearly in favor of the non-mature one at the end of the expression period, whereas Cdc50p in P3 membranes remained properly glycosylated. This suggested that Cdc50p in the P3 fraction has reached compartments where more complete maturation has occurred. We tested whether expression of Drs2p and Cdc50p in P3 or P2 membranes would result in different functional properties, taking advantage of the fact that P-type ATPases generally form a stable phosphorylated intermediate during their catalytic cycle. P3 and P2 membranes were thus subjected to phosphorylation from [γ–^{32}P]ATP and the amount of phosphoenzyme formed at steady state was measured, either in the presence or in the absence of vanadate, a potent inhibitor of P-type ATPases. As displayed in Fig. 6.9d, vanadate-sensitive phosphorylation was threefold to fourfold higher in P3 membranes than in P2 membranes, suggesting that the most active Drs2p was recovered in P3 membranes (Jacquot et al. 2012).

To estimate the concentration of Drs2p-BAD in P3 membranes, we made use of two additional samples, namely P3 membranes from yeast expressing Serca1a-BAD (~ 119 kDa; Cardi et al. 2010a) and P3 membranes from nontransformed yeast, supplemented with 1.5 % (w/w) of Serca1a-containing SR fragments (Fig. 6.10, "SR") where Serca1a is known to be the predominant protein. Firstly, comparison of both samples using the Ab79 antibody directed against Serca1a indicated that yeast membranes are enriched to about 1.5–2 % in Serca1a-BAD (Fig. 6.10, top blot). Secondly, comparison of the same Serca1a-BAD samples with Drs2p-BAD/Cdc50p-His_{10}-containing P3 membranes using a biotin probe indicated that for the same amount of total proteins present in P3 membranes, the amount of Drs2p-BAD is about twice that of Serca1a-BAD (Fig. 6.10, bottom blot). Thus, assuming that the BAD domains in Drs2p-BAD and Serca1a-BAD react similarly toward the biotin probe, Drs2p-BAD is expected to be enriched to about 3 % (w/w) relative to the amount of total proteins in P3 membranes. Hence, out of the 0.5 g of total proteins recovered in the P3 fraction for 1 liter of culture, 15 mg correspond to Drs2p.

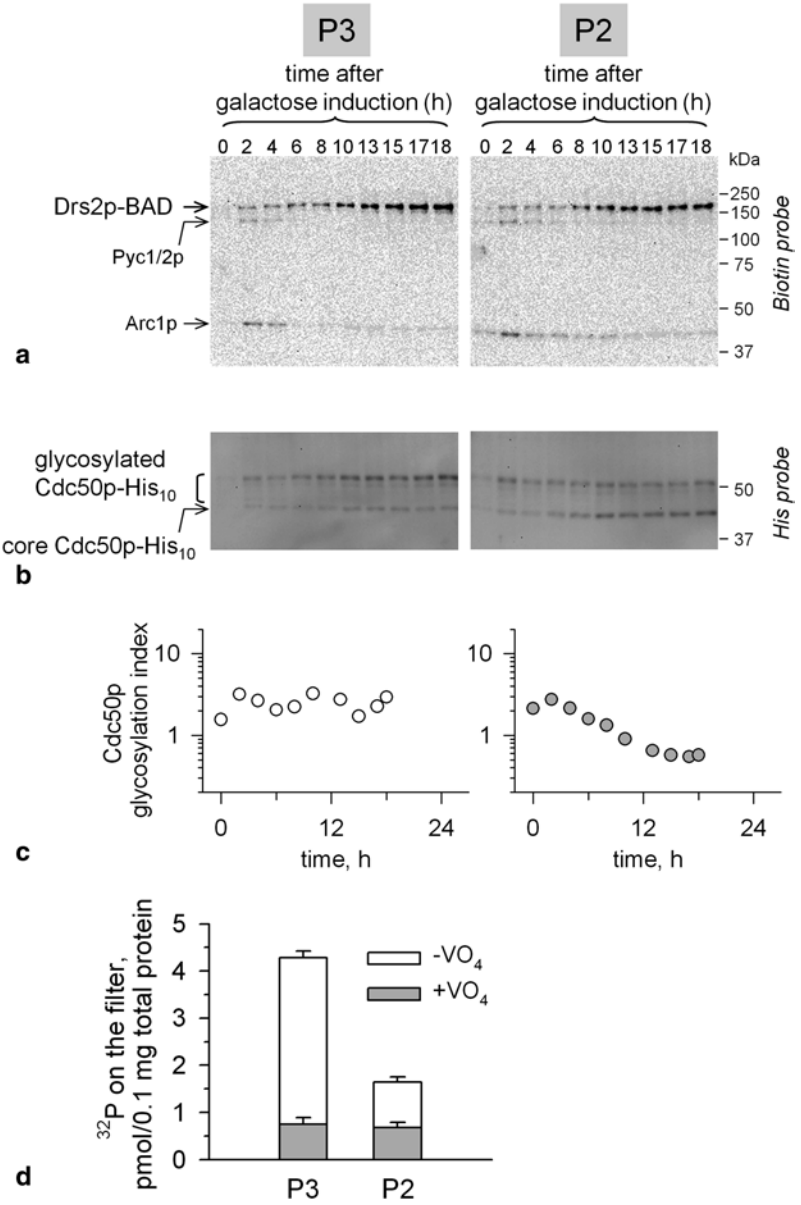

Fig. 6.9 Co-expression of Drs2p-BAD and Cdc50p-His_{10} in two types of yeast membranes. After various periods of induction by galactose, Drs2p-BAD and Cdc50p-His_{10} expressions in P3 and P2 membranes were analyzed by western blotting, after loading onto SDS-PAGE the same amount of total protein for each fraction (0.2–0.3 µg). **a** Drs2p-BAD was detected using a biotin probe. In the range of molecular masses illustrated, the biotin probe also weakly detects yeast proteins known to be biotinylated: acetyl-CoA carboxylase (Acc1p) at ~250 kDa (not clearly visible here), pyruvate carboxylase (Pyc1/2p) at ~130 kDa, and acyl-RNA complex (Arc1p) at ~42 kDa. **b** Cdc50p-His_{10} was detected using a His probe. The bands with various apparent molecular masses detected using the His probe correspond to various degrees of glycosylation of Cdc50p (Jacquot et al. 2012).

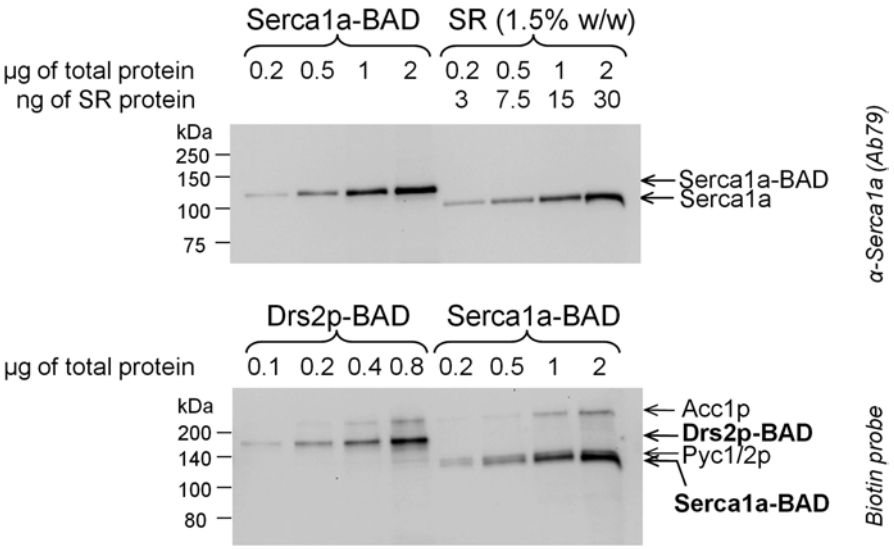

Fig. 6.10 Estimation of the concentration of Drs2p-BAD in P3 membranes of yeast overexpressing Drs2p-BAD/Cdc50p-His_{10}. The top gel compares P3 membranes derived from yeast cells expressing Serca1a-BAD with P3 membranes derived from nontransformed yeast cells, to which native sarcoplasmic reticulum (SR) membranes containing Serca1a were added (these SR membranes were mixed with the P3 membranes at a 1.5 % w/w ratio). The Serca1a content in native SR membranes is known to be about 4–6 nmol ATPase/mg total protein. Immunoblotting of the top gel was performed using a α-Serca1a antibody ("Ab79"). The bottom gel shows comparison of the same P3 membranes derived from yeast expressing Serca1a-BAD but now together with P3 membranes containing Drs2p-BAD/Cdc50p-His_{10}. Immunoblotting of the bottom gel was performed using a biotin probe

6.4.4 *Toward Purification of the Drs2p/Cdc50p Complex: Solubilization and Stability in Detergents*

In view of future purification of the Drs2p/Cdc50p complex, we investigated the ability of various detergents to solubilize Drs2p-BAD and Cdc50p-His_{10}. DDM, which among nonionic mild detergents proved appropriate for solubilizing Serca1a

c Evolution of Cdc50p glycosylation over induction time in both P2 and P3 membranes. Glycosylated and core *Cdc50p* were quantified using the "Quantity One" software, and the glycosylation index shown is the ratio between the fully glycosylated and the nonglycosylated forms. **d** Phosphorylation from [γ–^{32}P]ATP of P3 and P2 membrane fractions co-expressing Drs2p-BAD and Cdc50p-His_{10}. Formation of the phosphoenzyme intermediate was measured after incubation of P3 or P2 membranes (at 0.5 mg total protein per mL) with 0.5 µM [γ–^{32}P]ATP (0.25–1 mCi/µmol) for 25 s on ice, followed by acid quenching and filtration (see Jacquot et al. (2012) for detailed experimental procedures). Phosphorylation took place in the absence or presence of 1 mM vanadate (*open bars* and *gray bars*, respectively). Data are presented as the mean +/- SD of duplicates. Panel **d** has been reproduced from Jacquot et al. (2012)

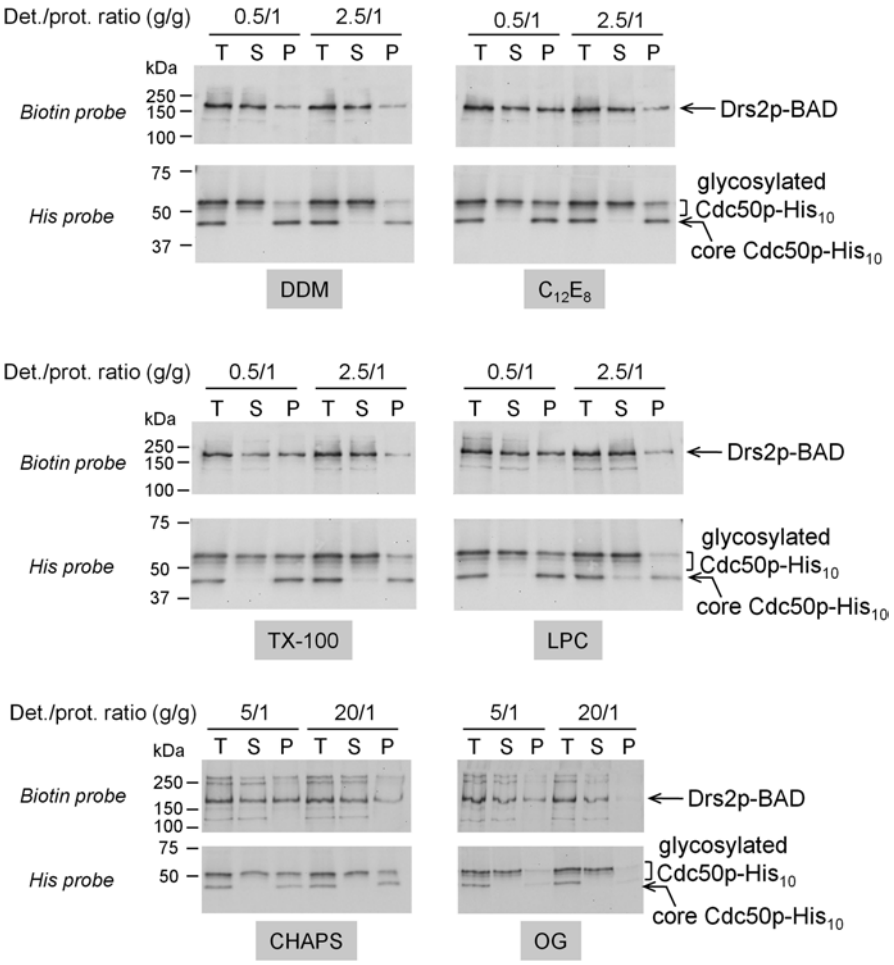

Fig. 6.11 Solubilization of P3 membranes with various detergents. P3 membranes containing Drs2p-BAD and Cdc50p-His_{10} were diluted to 2 mg proteins per mL in an ice-cold solubilization buffer supplemented with detergent (DDM, $C_{12}E_8$, TX-100, LPC, CHAPS, or OG), at the indicated detergent to protein ratio. After 1 h of incubation at 4 °C, detergent-treated membranes ("*T*") were centrifuged at 100,000 g for 1 h at 4 °C and soluble ("*S*") material was separated from the insoluble ("*P*") fraction. The "*P*" fraction was resuspended with solubilization buffer in the same volume as that of the "*T*" fraction. 0.5 µg of the "*T*" fraction was loaded onto SDS-PAGE and the same volumes of "*S*" and "*P*" fractions were loaded as well. Drs2p-BAD was detected using a biotin probe and Cdc50p-His_{10} was detected using a His probe. (Figure adapted from Jacquot et al. 2012)

expressed in yeast membranes (Lenoir et al. 2002; Jidenko et al. 2006), and $C_{12}E_8$, which up to now remains the favorite detergent for crystallization of P-type ATPases (Toyoshima et al. 2000; Pedersen et al. 2007; Gourdon et al. 2011), were included in this screen (Fig. 6.11). As can be seen from Fig. 6.11, DDM allowed almost complete solubilization of Drs2p-BAD (compare "T" for total and "S" for supernatant lanes) at DDM-to-protein ratios as low as 0.5 g/g. Solubilization with $C_{12}E_8$

proved to also be efficient, although perhaps slightly less than DDM, with about 50 % Drs2p-BAD solubilized for a 0.5 g/g detergent to protein ratio, while increasing this ratio to 2.5 g/g allowed almost complete solubilization of Drs2p-BAD. Triton X-100 (TX-100), another mild detergent, L-α-lysophosphatidylcholine (LPC), a zwitterionic detergent, or high critical micelle concentration (cmc) detergents like CHAPS and octyl-glucoside (OG) were also tested and turned out to solubilize Drs2p-BAD as efficiently as $C_{12}E_8$ (Fig. 6.11), although at higher concentrations for CHAPS and OG. Remarkably, the unglycosylated portion of Cdc50p-His_{10} remained insoluble in all cases, while solubilization of the glycosylated, mature form displayed a similar dependence on detergent concentration as that of Drs2p-BAD (Fig. 6.11; Jacquot et al. 2012).

The ability of these detergents to solubilize both Drs2p-BAD and the glycosylated portion of Cdc50p-His_{10} provided us with a tool for investigating whether both proteins interact with each other after solubilization. Indeed, incubating DDM-solubilized P3 membranes with Ni^{2+}-NTA beads, to fish out Cdc50p *via* its C-terminal decahistidine tag, indicated that both Cdc50p-His_{10} and Drs2p-BAD were retained to the beads and therefore that they do interact with each other after solubilization with detergent (not shown here, see (Jacquot et al. 2012)).

The choice of the detergent to be used for solubilization and purification of MPs remains largely empirical. A first approach consists in screening several detergents and trying to figure out at the end of the process which one is the most suitable for preserving the activity of the purified target. An alternative approach consists in setting up a functional assay already usable with crude membranes enriched with the protein of interest, to guide the screening of the many conceivable conditions for solubilization and purification. For this purpose, we resorted to phosphorylation of Drs2p from [γ–^{32}P]ATP. We first tested short-term effects of detergents; for such experiments, detergent was added to P3 membranes prepared from yeast co-expressing Cdc50p-His_{10} and Drs2p-BAD, and phosphorylation from [γ–^{32}P]ATP was measured after only short incubation in the presence of these detergents. Open bars in Fig. 6.12a show the phosphorylation levels measured for wild-type Drs2p while gray bars show the level for the inactive D560N mutant, the difference being characteristic of active Drs2p. Some of the detergents tested (all at a concentration above the cmc) left the phosphorylation level at a steady state essentially unaltered (e.g., $C_{12}E_8$ and CHAPS) while others like TX-100, digitonin, and diC_7PC led to rather low levels of phosphorylation. The phosphorylation level measured in the presence of DDM was even slightly higher than that measured in native membranes (Fig. 6.12a).

As detergents are not only known to alter the steady-state level of phosphorylation of P-type ATPases but also to make these MPs more prone to time-dependent inactivation (e.g., Lund et al. 1989), membranes were incubated with detergent for various periods of time before the phosphorylation measurement took place (Fig. 6.12b). Both $C_{12}E_8$ and TX-100 turned out to inactivate Drs2p rather rapidly, since phosphorylatability of Drs2p was almost completely lost after 3 h of incubation in those detergents (Fig. 6.12b, left panel), at variance with DDM, which made it possible to keep phosphorylatable a substantial fraction of Drs2p, even after several hours incubation. Using CHAPS, either in the absence or in the presence of

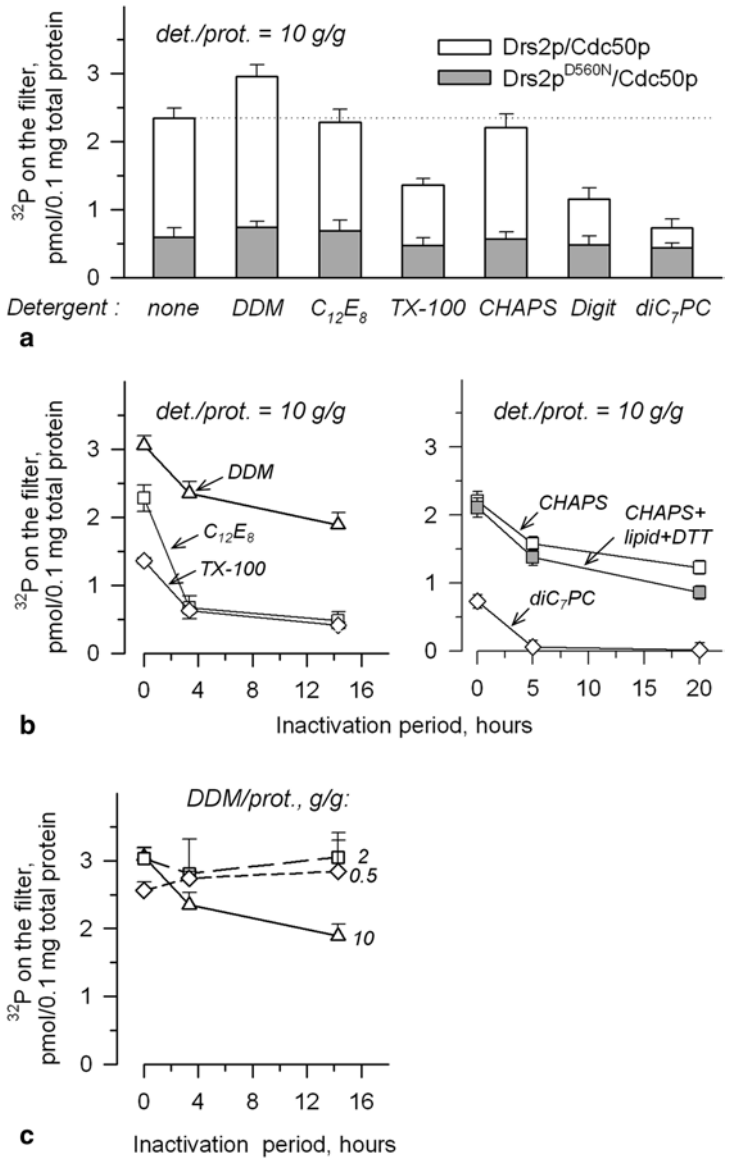

Fig. 6.12 Short-term and long-term effects of detergents on Drs2p/Cdc50p ability to become phosphorylated from ATP. P3 membranes containing either Drs2p-BAD/Cdc50p-His_{10} (*white bars*) or $Drs2p^{D560N}$-BAD/Cdc50p-His_{10} (*gray bars*) were suspended at 2 mg/ml in solubilization buffer. **a** Samples were incubated for 1 min in the presence of various detergents, all at 20 mg/mL. The detergents used are indicated (*Digit*, digitonin; *TX-100*, Triton X-100). Phosphorylation from [γ–^{32}P]ATP was then carried out as described in legend to Fig. 6.9. **b** For selected detergents, similar measurements were made after incubation on ice for various periods of time. **c** *DDM* was tested at various concentrations, resulting in various detergent-to-protein ratios. Data are presented as the mean+/- SD ($n=3$). (Figure adapted from Jacquot et al. 2012)

egg lecithin and DTT (Coleman et al. 2009), did not improve stability of the Drs2p/Cdc50p complex (Fig. 6.12b, right panel). The short-chain lipid diC_7PC, previously described not to be toxic in the case of a number of other MPs (e.g., see Hauser 2000), was very poor at preserving Drs2p from inactivation (Fig. 6.12b, right panel). Adding selected lipids together with detergent protected the ability of Drs2p to become phosphorylated (data not shown).

Although phosphorylation is not a true indicator of enzyme turnover, this suggested that DDM might be a good candidate for further purification of the complex. We thus explored whether reducing the detergent to protein ratio (from 10 to 2 or 0.5 g/g) would help maintaining Drs2p phosphorylation at its initial level for longer incubation periods. As displayed in Fig. 6.12c, lower detergent to protein ratios (but still solubilizing ones, see Fig. 6.11) indeed kept Drs2p stable over hours of incubation on ice, probably as a result of a less dramatic delipidation of the hydrophobic surface of the protein.

6.5 Conclusions

The overexpression system described in this chapter has thus been successful for crystallization of a mammalian MP, the Serca1a Ca^{2+}-ATPase, as well as for the coordinated expression of the yeast Drs2p/Cdc50p complex (Jidenko et al. 2005; Jacquot et al. 2012). For the latter, the next stage will consist in purifying the complex in a functional form to gain insights into the molecular mechanism for lipid transport.

Beyond the examples of rabbit Serca1a and of yeast Drs2p/Cdc50p complex, overexpression in *S. cerevisiae* of other MPs has been attempted (see Table 6.2 for details). For instance, the human cardiac Ca^{2+}-ATPase Serca2a was overexpressed using our system and purified by single-step affinity chromatography (Antaloae et al. 2013).

In our laboratory, another Ca^{2+}-ATPase has been subjected to heterologous expression in *S. cerevisiae,* namely PfATP6, a Ca^{2+}-ATPase from *Plasmodium falciparum*. After overexpression, the purification yield of PfATP6 is similar to that of the rabbit Serca1a, and although the two proteins share a rather high degree of sequence similarity they exhibit significant differences with respect to their sensitivity to known SERCA inhibitors, e.g., thapsigargin and cyclopiazonic acid (Cardi et al. 2010b; Arnou et al. 2011). At variance with studies from others, our work demonstrated that PfATP6 is probably not the target of the antimalarial drug artemisinin; recently, our purified recombinant PfATP6 was used for screening from a compound library inhibitors that might potentially be used as new antimalarial drugs (David-Bosne et al. 2013).

Also, we did not restrict our system to overexpression of P-type ATPases. A transporter that belongs to the mitochondrial carrier family (MCF), the human ADP/ATP translocase AAC1 (see, for instance, Nury et al. 2006 for review), was overexpressed in *S. cerevisiae*. The expression level of AAC1 is about twice higher than that of Serca1a and after purification, AAC1 is functional with respect to

Table 6.2 Membrane proteins successfully expressed using the pYeDP60/BAD system

Protein names and functions	Organism and organelle	Number of TM	MW, kDa	Specific features and comments	References
Ca^{2+} transporters					
Serca1a	Rabbit, ER	10	110	WT and mutants	Centeno et al. 1994; Lenoir et al. 2002; Jidenko et al. 2006; Cardi 2010a
Serca2a	Human, ER	10	115	WT	Antaloae et al. 2013
PfATP6	*P. falciparum,* ER	10 (?)	140	WT	Cardi et al. 2010b; Arnou et al. 2011; David-Bosne et al. 2013
Lipid transporter					
Drs2p/Cdc50p complex	Yeast, TGN	10/2 (?)	150/40	WT and mutants/ glycosylated (Cdc50p)	Jacquot et al. 2012
ADP/ATP translocase					
hAAC1	Human, Mitochondria	6	33		
K^+ channel					
TREK-1	Mouse, PM	4–6 (?)	47	Glycosylated	Berrier et al. 2013

binding of substrates and inhibitors (unpublished results). The two-pore domain eukaryotic K^+ channel TREK-1, that plays an essential role in setting the neuronal membrane potential, was also successfully expressed, purified, and reconstituted in proteoliposomes. Subsequent electrophysiological recordings on the reconstituted protein established that TREK-1 is a mechanosensitive channel directly sensitive to a change in membrane tension (Berrier et al. 2013).

At the present time, the high-resolution structure of these MPs (beyond Serca1a) has not been solved, but for some of them, crystallization trials are in progress.

Acknowledgments We wish to thank Raphaëlle Barry for her initial help in the "flippase" project, and specifically for construction of the co-expression plasmid, and Stéphanie David-Bosne for stimulating discussions.

This work was supported by the French Infrastructure for Integrated Structural Biology (FRISBI) and by grants from the Agence Nationale pour la Recherche and the Ile de France region (Domaine d'Intérêt Majeur Maladies Infectieuses, DIM MALINF).

References

Alder-Baerens N, Lisman Q, Luong L, Pomorski T, Holthuis JC (2006) Loss of P4 ATPases Drs2p and Dnf3p disrupts aminophospholipid transport and asymmetry in yeast post-Golgi secretory vesicles. Mol Biol Cell 17:1632–1642

Andersen JP (1995) Dissection of the functional domains of the sarcoplasmic reticulum Ca^{2+}-ATPase by site-directed mutagenesis. Biosci Rep 15:243–261

Andersen JP, Vilsen B (1992) Functional consequences of alterations to Glu309, Glu771, and Asp800 in the Ca^{2+}-ATPase of sarcoplasmic reticulum. J Biol Chem 267:19383–19387

Antaloae AV, Montigny C, le Maire M, Watson KA, Sorensen TL (2013) Optimisation of recombinant production of active human cardiac SERCA2a ATPase. PLoS One 8:e71842

Arnou B, Montigny C, Morth JP, Nissen P, Jaxel C, Moller JV, Maire M (2011) The Plasmodium falciparum Ca^{2+}-ATPase PfATP6: insensitive to artemisinin, but a potential drug target. Biochem Soc Trans 39:823–831

Arsenieva D, Symersky J, Wang Y, Pagadala V, Mueller DM (2010) Crystal structures of mutant forms of the yeast F1 ATPase reveal two modes of uncoupling. J Biol Chem 285:36561–36569

Berrier C, Pozza A, de Lacroix deLA, Chardonnet S, Mesneau A, Jaxel C, le Maire M, Ghazi A (2013) The purified mechanosensitive channel TREK-1 is directly sensitive to membrane tension. J Biol Chem 288(38):27307–27314

Bigelow DJ, Inesi G (1992) Contributions of chemical derivatization and spectroscopic studies to the characterization of the Ca^{2+} transport ATPase of sarcoplasmic reticulum. Biochim Biophys Acta 1113:323–338

Bill RM, Henderson PJ, Iwata S, Kunji ER, Michel H, Neutze R, Newstead S, Poolman B, Tate CG, Vogel H (2011) Overcoming barriers to membrane protein structure determination. Nat Biotechnol 29:335–340

Binda C, Newton-Vinson P, Hubalek F, Edmondson DE, Mattevi A (2002) Structure of human monoamine oxidase B, a drug target for the treatment of neurological disorders. Nat Struct Biol 9:22–26

Blagovic B, Rupcic J, Mesaric M, Georgiu K, Maric V (2001) Lipid composition of brewer's yeast. Food Technol Biotechnol 39:175–181

Blagovic B, Rupcic J, Mesaric M, Maric V (2005) Lipid analysis of the plasma membrane and mitochondria of brewer's yeast. Folia Microbiol (Praha) 50:24–30

Bleve G, Di Sansebastiano GP, Grieco F (2011) Over-expression of functional *Saccharomyces cerevisiae* GUP1, induces proliferation of intracellular membranes containing ER and Golgi resident proteins. Biochim Biophys Acta 1808:733–744

Brachmann CB, Davies A, Cost GJ, Caputo E, Li J, Hieter P, Boeke JD (1998) Designer deletion strains derived from *Saccharomyces cerevisiae* S288C: a useful set of strains and plasmids for PCR-mediated gene disruption and other applications. Yeast 14:115–132

Brandl CJ, Green NM, Korczak B, MacLennan DH (1986) Two Ca^{2+} ATPase genes: homologies and mechanistic implications of deduced amino acid sequences. Cell 44:597–607

Britton Z, Young C, Can O, McNeely P, Naranjo A, Robinson A (2011) Membrane protein expression in *Saccharomyces cerevisiae*. In: Robinson A (ed) Production of membrane proteins: strategies for production and isolation. Wiley-VCH, Weinheim

Bryde S, Hennrich H, Verhulst PM, Devaux PF, Lenoir G, Holthuis JC (2010) CDC50 proteins are critical components of the human class-1 P4-ATPase transport machinery. J Biol Chem 285:40562–40572

Bull LN, van Eijk MJ, Pawlikowska L, DeYoung JA, Juijn JA, Liao M, Klomp LW, Lomri N, Berger R, Scharschmidt BF, Knisely AS, Houwen RH, Freimer NB (1998) A gene encoding a P-type ATPase mutated in two forms of hereditary cholestasis. Nat Genet 18:219–224

Canadi Juresic G, Blagovic B (2011) The influence of fermentation conditions and recycling on the phospholipid and fatty acid composition of the brewer's yeast plasma membranes. Folia Microbiol (Praha) 56:215–224

Cardi D, Montigny C, Arnou B, Jidenko M, Marchal E, le Maire M, Jaxel C (2010a) Heterologous expression and affinity purification of eukaryotic membrane proteins in view of functional and structural studies: the example of the sarcoplasmic reticulum Ca^{2+}-ATPase. Method Mol Biol 601:247–267

Cardi D, Pozza A, Arnou B, Marchal E, Clausen JD, Andersen JP, Krishna S, Moller JV, le Maire M, Jaxel C (2010b) Purified E255 L mutant SERCA1a and purified PfATP6 are sensitive to SERCA-type inhibitors but insensitive to artemisinins. J Biol Chem 285:26406–26416

Carpenter EP, Beis K, Cameron AD, Iwata S (2008) Overcoming the challenges of membrane protein crystallography. Curr Opin Struct Biol 18:581–586

Celik E, Calik P (2012) Production of recombinant proteins by yeast cells. Biotechnol Adv 30:1108–1118

Centeno F, Deschamps S, Lompre AM, Anger M, Moutin MJ, Dupont Y, Palmgren MG, Villalba JM, Moller JV, Falson P et al (1994) Expression of the sarcoplasmic reticulum Ca^{2+}-ATPase in yeast. FEBS Lett 354:117–122

Chapman-Smith A, Cronan JE Jr (1999) The enzymatic biotinylation of proteins: a post-translational modification of exceptional specificity. Trends Biochem Sci 24:359–363

Chen CY, Ingram MF, Rosal PH, Graham TR (1999) Role for Drs2p, a P-type ATPase and potential aminophospholipid translocase, in yeast late Golgi function. J Cell Biol 147:1223–1236

Chen S, Wang J, Muthusamy BP, Liu K, Zare S, Andersen RJ, Graham TR (2006) Roles for the Drs2p-Cdc50p complex in protein transport and phosphatidylserine asymmetry of the yeast plasma membrane. Traffic 7:1503–1517

Chiba Y, Akeboshi H (2009) Glycan engineering and production of 'humanized' glycoprotein in yeast cells. Biol Pharm Bull 32:786–795

Chiba Y, Jigami Y (2007) Production of humanized glycoproteins in bacteria and yeasts. Curr Opin Chem Biol 11:670–676

Clarke DM, Loo TW, Inesi G, MacLennan DH (1989) Location of high affinity Ca^{2+}-binding sites within the predicted transmembrane domain of the sarcoplasmic reticulum Ca^{2+}-ATPase. Nature 339:476–478

Coleman JA, Kwok MC, Molday RS (2009) Localization, purification, and functional reconstitution of the P4-ATPase Atp8a2, a phosphatidylserine flippase in photoreceptor disc membranes. J Biol Chem 284:32670–32679

Coleman JA, Quazi F, Molday RS (2012) Mammalian P4-ATPases and ABC transporters and their role in phospholipid transport. Biochim Biophys Acta 1831:555–574

Consler TG, Persson BL, Jung H, Zen KH, Jung K, Prive GG, Verner GE, Kaback HR (1993) Properties and purification of an active biotinylated lactose permease from *Escherichia coli*. Proc Natl Acad Sci U S A 90:6934–6938

Cronan JE Jr (1990) Biotination of proteins in vivo. A post-translational modification to label, purify, and study proteins. J Biol Chem 265:10327–10333

Daleke DL (2007) Phospholipid flippases. J Biol Chem 282:821–825

Daum G, Tuller G, Nemec T, Hrastnik C, Balliano G, Cattel L, Milla P, Rocco F, Conzelmann A, Vionnet C, Kelly DE, Kelly S, Schweizer E, Schuller HJ, Hojad U, Greiner E, Finger K (1999) Systematic analysis of yeast strains with possible defects in lipid metabolism. Yeast 15:601–614

David-Bosne S, Florent I, Lund-Winther AM, Hansen JB, Buch-Pedersen M, Machillot P, le Maire M, Jaxel C (2013) Antimalarial screening via large-scale purification of *Plasmodium falciparum* Ca^{2+}-ATPase 6 and in vitro studies. FEBS J 280(21):5419–5429

Decottignies A, Grant AM, Nichols JW, de Wet H, McIntosh DB, Goffeau A (1998) ATPase and multidrug transport activities of the overexpressed yeast ABC protein Yor1p. J Biol Chem 273:12612–12622

Degani C, Boyer PD (1973) A borohydride reduction method for characterization of the acyl phosphate linkage in proteins and its application to sarcoplasmic reticulum adenosine triphosphatase. J Biol Chem 248:8222–8226

Diers IV, Rasmussen E, Larsen PH, Kjaersig IL (1991) Yeast fermentation processes for insulin production. Bioprocess Technol 13:166–76.

Devaux PF, Herrmann A, Ohlwein N, Kozlov MM (2008) How lipid flippases can modulate membrane structure. Biochim Biophys Acta 1778:1591–1600

Dux L, Martonosi A (1983) Two-dimensional arrays of proteins in sarcoplasmic reticulum and purified Ca^{2+}-ATPase vesicles treated with vanadate. J Biol Chem 258:2599–2603

Ebashi S, Lipmann F (1962) Adenosine triphosphate-linked concentration of calcium Ions in a particulate fraction of rabbit muscle. J Cell Biol 14:389–400

Fadok VA, Bratton DL, Rose DM, Pearson A, Ezekewitz RA, Henson PM (2000) A receptor for phosphatidylserine-specific clearance of apoptotic cells. Nature 405:85–90

Furuta N, Fujimura-Kamada K, Saito K, Yamamoto T, Tanaka K (2007) Endocytic recycling in yeast is regulated by putative phospholipid translocases and the Ypt31p/32p-Rcy1p pathway. Mol Biol Cell 18:295–312

Gall WE, Geething NC, Hua Z, Ingram MF, Liu K, Chen SI, Graham TR (2002) Drs2p-dependent formation of exocytic clathrin-coated vesicles in vivo. Curr Biol 12:1623–1627

Gemmill TR, Trimble RB (1999) Overview of N- and O-linked oligosaccharide structures found in various yeast species. Biochim Biophys Acta 1426:227–237

Goffeau A, Barrell BG, Bussey H, Davis RW, Dujon B, Feldmann H, Galibert F, Hoheisel JD, Jacq C, Johnston M, Louis EJ, Mewes HW, Murakami Y, Philippsen P, Tettelin H, Oliver SG (1996) Life with 6000 genes. Science 274(546):563–547

Gourdon P, Liu XY, Skjorringe T, Morth JP, Moller LB, Pedersen BP, Nissen P (2011) Crystal structure of a copper-transporting PIB-type ATPase. Nature 475:59–64

Graham TR (2004) Flippases and vesicle-mediated protein transport. Trends Cell Biol 14:670–677

Griffith DA, Delipala C, Leadsham J, Jarvis SM, Oesterhelt D (2003) A novel yeast expression system for the overproduction of quality-controlled membrane proteins. FEBS Lett 553:45–50

Grisshammer R, Tate CG (1995) Overexpression of integral membrane proteins for structural studies. Q Rev Biophys 28:315–422

Guarente L, Yocum RR, Gifford P (1982) A *GAL10–CYC1* hybrid yeast promoter identifies the *GAL4* regulatory region as an upstream site. Proc Natl Acad Sci U S A 79:7410–7414

Gunge N (1983) Yeast DNA plasmids. Annu Rev Microbiol 37:253–276

Hasselbach W, Makinose M (1961) [The calcium pump of the "relaxing granules" of muscle and its dependence on ATP-splitting]. Biochem Z 333:518–528

Hauser H (2000) Short-chain phospholipids as detergents. Biochim Biophys Acta 1508:164–181

Haviv H, Habeck M, Kanai R, Toyoshima C, Karlish SJ (2013) Neutral phospholipids stimulate Na, K-ATPase activity: a specific lipid-protein interaction. J Biol Chem 288:10073–10081

Helenius A, Aebi M (2001) Intracellular functions of N-linked glycans. Science 291:2364–2369

Howard EM, Roepe PD (2003) Purified human MDR 1 modulates membrane potential in reconstituted proteoliposomes. Biochemistry 42:3544–3555

Hua Z, Fatheddin P, Graham TR (2002) An essential subfamily of Drs2p-related P-type ATPases is required for protein trafficking between Golgi complex and endosomal/vacuolar system. Mol Biol Cell 13:3162–3177

Jacquot A, Montigny C, Hennrich H, Barry R, le Maire M, Jaxel C, Holthuis J, Champeil P, Lenoir G (2012) Stimulation by phosphatidylserine of Drs2p/Cdc50p lipid translocase dephosphorylation is controlled by phoshatidylinositol-4-phosphate. J Biol Chem 287:13249–13261

Jidenko M, Nielsen RC, Sorensen TL, Moller JV, le Maire M, Nissen P, Jaxel C (2005) Crystallization of a mammalian membrane protein overexpressed in *Saccharomyces cerevisiae*. Proc Natl Acad Sci U S A 102:11687–11691

Jidenko M, Lenoir G, Fuentes JM, le Maire M, Jaxel C (2006) Expression in yeast and purification of a membrane protein, SERCA1a, using a biotinylated acceptor domain. Protein Expr Purif 48:32–42

Kapri-Pardes E, Katz A, Haviv H, Mahmmoud Y, Ilan M, Khalfin-Penigel I, Carmeli S, Yarden O, Karlish SJ (2011) Stabilization of the alpha2 isoform of Na, K-ATPase by mutations in a phospholipid binding pocket. J Biol Chem 286:42888–42899

Kellosalo J, Kajander T, Kogan K, Pokharel K, Goldman A (2012a) The structure and catalytic cycle of a sodium-pumping pyrophosphatase. Science 337:473–476

Kellosalo J, Kajander T, Honkanen R, Goldman A (2012b) Crystallization and preliminary X-ray analysis of membrane-bound pyrophosphatases. Mol Membr Biol 30:64–74

Kinnunen PK, Holopainen JM (2000) Mechanisms of initiation of membrane fusion: role of lipids. Biosci Rep 20:465–482

Kitson SM, Mullen W, Cogdell RJ, Bill RM, Fraser NJ (2011) GPCR production in a novel yeast strain that makes cholesterol-like sterols. Methods 55:287–292

Lagane B, Gaibelet G, Meilhoc E, Masson JM, Cezanne L, Lopez A (2000) Role of sterols in modulating the human mu-opioid receptor function in *Saccharomyces cerevisiae*. J Biol Chem 275:33197–33200

Lander ES, Linton LM, Birren B, Nusbaum C, Zody MC, Baldwin J, Devon K, Dewar K, Doyle M, FitzHugh W, Funke R et al (2001) Initial sequencing and analysis of the human genome. Nature 409:860–921

Lee KM, DaSilva NA (2005) Evaluation of the *Saccharomyces cerevisiae* ADH2 promoter for protein synthesis. Yeast 22:431–440

Lee AG, East JM (1998) The effects of phospholipid structure on the function of a calcium pump. Biochem Soc Trans 26:359–365

Lee JK, Stroud RM (2010) Unlocking the eukaryotic membrane protein structural proteome. Curr Opin Struct Biol 20:464–470

Lenoir G, Menguy T, Corre F, Montigny C, Pedersen PA, Thines D, le Maire M, Falson P (2002) Overproduction in yeast and rapid and efficient purification of the rabbit SERCA1a Ca^{2+}-ATPase. Biochim Biophys Acta 1560:67–83

Lenoir G, Picard M, Moller JV, le Maire M, Champeil P, Falson P (2004) Involvement of the L6-7 loop in SERCA1a Ca^{2+}-ATPase activation by Ca^{2+} (or Sr^{2+}) and ATP. J Biol Chem 279:32125–32133

Lenoir G, Jaxel C, Picard M, le Maire M, Champeil P, Falson P (2006) Conformational changes in sarcoplasmic reticulum Ca^{2+}-ATPase mutants: effect of mutations either at Ca^{2+}-binding site II or at tryptophan 552 in the cytosolic domain. Biochemistry 45:5261–5270

Lenoir G, Williamson P, Holthuis JC (2007) On the origin of lipid asymmetry: the flip side of ion transport. Curr Opin Chem Biol 11:654–661

Lenoir G, Williamson P, Puts CF, Holthuis JC (2009) Cdc50p plays a vital role in the ATPase reaction cycle of the putative aminophospholipid transporter drs2p. J Biol Chem 284:17956–17967

Li WZ, Sherman F (1991) Two types of TATA elements for the *CYC1* gene of the yeast *Saccharomyces cerevisiae*. Mol Cell Biol 11:666–676

Li M, Hays FA, Roe-Zurz Z, Vuong L, Kelly L, Ho CM, Robbins RM, Pieper U, O'Connell JD 3rd, Miercke LJ, Giacomini KM, Sali A, Stroud RM (2009) Selecting optimum eukaryotic integral membrane proteins for structure determination by rapid expression and solubilization screening. J Mol Biol 385:820–830

Lin SM, Tsai JY, Hsiao CD, Huang YT, Chiu CL, Liu MH, Tung JY, Liu TH, Pan RL, Sun YJ (2012) Crystal structure of a membrane-embedded H^+-translocating pyrophosphatase. Nature 484:399–403

Long SB, Campbell EB, Mackinnon R (2005) Crystal structure of a mammalian voltage-dependent Shaker family K^+ channel. Science 309:897–903

Lopez-Marques RL, Holthuis JC, Pomorski TG (2011) Pumping lipids with P4-ATPases. Biol Chem 392:67–76

Lund S, Orlowski S, de Foresta B, Champeil P, le Maire M, Moller JV (1989) Detergent structure and associated lipid as determinants in the stabilization of solubilized Ca^{2+}-ATPase from sarcoplasmic reticulum. J Biol Chem 264:4907–4915

Ma J, Ito A (2002) Tyrosine residues near the FAD binding site are critical for FAD binding and for the maintenance of the stable and active conformation of rat monoamine oxidase A. J Biochem 131:107–111

Ma J, Yoshimura M, Yamashita E, Nakagawa A, Ito A, Tsukihara T (2004a) Structure of rat monoamine oxidase A and its specific recognitions for substrates and inhibitors. J Mol Biol 338:103–114

Ma J, Kubota F, Yoshimura M, Yamashita E, Nakagawa A, Ito A, Tsukihara T (2004b) Crystallization and preliminary crystallographic analysis of rat monoamine oxidase A complexed with clorgyline. Acta Crystallogr D Biol Crystallogr 60:317–319

Marchand A, Winther AM, Holm PJ, Olesen C, Montigny C, Arnou B, Champeil P, Clausen JD, Vilsen B, Andersen JP, Nissen P, Jaxel C, Moller JV, le Maire M (2008) Crystal structure of D351A and P312A mutant forms of the mammalian sarcoplasmic reticulum $Ca2^+$ -ATPase reveals key events in phosphorylation and Ca^{2+} release. J Biol Chem 283:14867–14882

Maruyama K, MacLennan DH (1988) Mutation of aspartic acid-351, lysine-352, and lysine-515 alters the Ca^{2+} transport activity of the Ca^{2+}-ATPase expressed in COS-1 cells. Proc Natl Acad Sci U S A 85:3314–3318

McAleer WJ, Buynak EB, Maigetter RZ, Wampler DE, Miller WJ, Hilleman MR (1984) Human hepatitis B vaccine from recombinant yeast. Nature 307:178–180

Mercer J, Helenius A (2008) Vaccinia virus uses macropinocytosis and apoptotic mimicry to enter host cells. Science 320:531–535

Meusser B, Hirsch C, Jarosch E, Sommer T (2005) ERAD: the long road to destruction. Nat Cell Biol 7:766–772

Midgett CR, Madden DR (2007) Breaking the bottleneck: eukaryotic membrane protein expression for high-resolution structural studies. J Struct Biol 160:265–274

Miras R, Cuillel M, Catty P, Guillain F, Mintz E (2001) Purification of heterologous sarcoplasmic reticulum Ca^{2+}-ATPase Serca1a allowing phosphoenzyme and Ca^{2+}-affinity measurements. Protein Expr Purif 22:299–306

Morth JP, Pedersen BP, Toustrup-Jensen MS, Sorensen TL, Petersen J, Andersen JP, Vilsen B, Nissen P (2007) Crystal structure of the sodium-potassium pump. Nature 450:1043–1049

Mueller DM, Puri N, Kabaleeswaran V, Terry C, Leslie AG, Walker JE (2004) Ni-chelate-affinity purification and crystallization of the yeast mitochondrial F1-ATPase. Protein Expr Purif 37:479–485

Nagy Z, Montigny C, Leverrier P, Yeh S, Goffeau A, Garrigos M, Falson P (2006) Role of the yeast ABC transporter Yor1p in cadmium detoxification. Biochimie 88:1665–1671

Natarajan P, Wang J, Hua Z, Graham TR (2004) Drs2p-coupled aminophospholipid translocase activity in yeast Golgi membranes and relationship to in vivo function. Proc Natl Acad Sci U S A 101:10614–10619

Nury H, Dahout-Gonzalez C, Trezeguet V, Lauquin GJ, Brandolin G, Pebay-Peyroula E (2006) Relations between structure and function of the mitochondrial ADP/ATP carrier. Annu Rev Biochem 75:713–741

Olesen C, Picard M, Winther AM, Gyrup C, Morth JP, Oxvig C, Moller JV, Nissen P (2007) The structural basis of calcium transport by the calcium pump. Nature 450:1036–1042

Op den Kamp JA (1979) Lipid asymmetry in membranes. Annu Rev Biochem 48:47–71

Osterberg M, Kim H, Warringer J, Melen K, Blomberg A, von Heijne G (2006) Phenotypic effects of membrane protein overexpression in *Saccharomyces cerevisiae*. Proc Natl Acad Sci U S A 103:11148–11153

Pagadala V, Vistain L, Symersky J, Mueller DM (2011) Characterization of the mitochondrial ATP synthase from yeast *Saccharomyces cerevisae*. J Bioenerg Biomembr 43:333–347

Paulusma CC, Folmer DE, Ho-Mok KS, de Waart DR, Hilarius PM, Verhoeven AJ, Oude Elferink RP (2008) ATP8B1 requires an accessory protein for endoplasmic reticulum exit and plasma membrane lipid flippase activity. Hepatology 47:268–278

Pedersen PA, Rasmussen JH, Joorgensen PL (1996) Expression in high yield of pig alpha 1 beta 1 Na, K-ATPase and inactive mutants D369N and D807N in *Saccharomyces cerevisiae*. J Biol Chem 271:2514–2522

Pedersen BP, Buch-Pedersen MJ, Morth JP, Palmgren MG, Nissen P (2007) Crystal structure of the plasma membrane proton pump. Nature 450:1111–1114

Pedersen BP, Kumar H, Waight AB, Risenmay AJ, Roe-Zurz Z, Chau BH, Schlessinger A, Bonomi M, Harries W, Sali A, Johri AK, Stroud RM (2013) Crystal structure of a eukaryotic phosphate transporter. Nature 496:533–536

Pomorski T, Lombardi R, Riezman H, Devaux PF, van Meer G, Holthuis JC (2003) Drs2p-related P-type ATPases Dnf1p and Dnf2p are required for phospholipid translocation across the yeast plasma membrane and serve a role in endocytosis. Mol Biol Cell 14:1240–1254

Pompon D (1988) cDNA cloning and functional expression in yeast *Saccharomyces cerevisiae* of beta-naphthoflavone-induced rabbit liver P-450 LM4 and LM6. Eur J Biochem 177:285–293

Pompon D, Louerat B, Bronine A, Urban P (1996) Yeast expression of animal and plant P450s in optimized redox environments. Method Enzymol 272:51–64

Poulsen LR, Lopez-Marques RL, McDowell SC, Okkeri J, Licht D, Schulz A, Pomorski T, Harper JF, Palmgren MG (2008a) The *Arabidopsis* P4-ATPase ALA3 localizes to the Golgi and requires a beta-subunit to function in lipid translocation and secretory vesicle formation. Plant Cell 20:658–676

Poulsen LR, Lopez-Marques RL, Palmgren MG (2008b) Flippases: still more questions than answers. Cell Mol Life Sci 65:3119–3125

Pouny Y, Weitzman C, Kaback HR (1998) In vitro biotinylation provides quantitative recovery of highly purified active lactose permease in a single step. Biochemistry 37:15713–15719

Powl AM, East JM, Lee AG (2008) Importance of direct interactions with lipids for the function of the mechanosensitive channel MscL. Biochemistry 47:12175–12184

Prive GG (2007) Detergents for the stabilization and crystallization of membrane proteins. Methods 41:388–397

Pryor EE Jr, Horanyi PS, Clark KM, Fedoriw N, Connelly SM, Koszelak-Rosenblum M, Zhu G, Malkowski MG, Wiener MC, Dumont ME (2013) Structure of the integral membrane protein CAAX protease Ste24p. Science 339:1600–1604

Puts CF, Panatala R, Hennrich H, Tsareva A, Williamson P, Holthuis JC (2012) Mapping functional interactions in a heterodimeric phospholipid pump. J Biol Chem 287:30529–30540

Romanos MA, Scorer CA, Clare JJ (1992) Foreign gene expression in yeast: a review. Yeast 8:423–488

Rosing J, Tans G, Govers-Riemslag JW, Zwaal RF, Hemker HC (1980) The role of phospholipids and factor Va in the prothrombinase complex. J Biol Chem 255:274–283

Saito K, Fujimura-Kamada K, Furuta N, Kato U, Umeda M, Tanaka K (2004) Cdc50p, a protein required for polarized growth, associates with the Drs2p P-type ATPase implicated in phospholipid translocation in *Saccharomyces cerevisiae*. Mol Biol Cell 15:3418–3432

Schultz LD, Hofmann KJ, Mylin LM, Montgomery DL, Ellis RW, Hopper JE (1987) Regulated overproduction of the *GAL4* gene product greatly increases expression from galactose-inducible promoters on multi-copy expression vectors in yeast. Gene 61:123–133

Schwarz E, Oesterhelt D, Reinke H, Beyreuther K, Dimroth P (1988) The sodium ion translocating oxalacetate decarboxylase of *Klebsiella pneumoniae*. Sequence of the biotin-containing alpha-subunit and relationship to other biotin-containing enzymes. J Biol Chem 263:9640–9645

Shinoda T, Ogawa H, Cornelius F, Toyoshima C (2009) Crystal structure of the sodium-potassium pump at 2.4 A resolution. Nature 459:446–450

Son SY, Ma J, Kondou Y, Yoshimura M, Yamashita E, Tsukihara T (2008) Structure of human monoamine oxidase A at 2.2-A resolution: the control of opening the entry for substrates/inhibitors. Proc Natl Acad Sci U S A 105:5739–5744

Sorensen TL, Moller JV, Nissen P (2004) Phosphoryl transfer and calcium ion occlusion in the calcium pump. Science 304:1672–1675

Sorensen TL, Olesen C, Jensen AM, Moller JV, Nissen P (2006) Crystals of sarcoplasmic reticulum Ca^{2+}-ATPase. J Biotechnol 124:704–716

Stock D, Leslie AG, Walker JE (1999) Molecular architecture of the rotary motor in ATP synthase. Science 286:1700–1705

Stolz J, Darnhofer-Demar B, Sauer N (1995) Rapid purification of a functionally active plant sucrose carrier from transgenic yeast using a bacterial biotin acceptor domain. FEBS Lett 377:167–171

Strock C, Cavagna M, Peiffer WE, Sumbilla C, Lewis D, Inesi G (1998) Direct demonstration of Ca^{2+} binding defects in sarco-endoplasmic reticulum Ca^{2+} ATPase mutants overexpressed in COS-1 cells transfected with adenovirus vectors. J Biol Chem 273:15104–15109

Toyoshima C, Nomura H (2002) Structural changes in the calcium pump accompanying the dissociation of calcium. Nature 418:605–611

Toyoshima C, Sasabe H, Stokes DL (1993) Three-dimensional cryo-electron microscopy of the calcium ion pump in the sarcoplasmic reticulum membrane. Nature 362:467–471

Toyoshima C, Nakasako M, Nomura H, Ogawa H (2000) Crystal structure of the calcium pump of sarcoplasmic reticulum at 2.6 A resolution. Nature 405:647–655

Toyoshima C, Norimatsu Y, Iwasawa S, Tsuda T, Ogawa H (2007) How processing of aspartylphosphate is coupled to lumenal gating of the ion pathway in the calcium pump. Proc Natl Acad Sci U S A 104:19831–19836

van der Velden LM, Wichers CG, van Breevoort AE, Coleman JA, Molday RS, Berger R, Klomp LW, van deGSF (2010) Heteromeric interactions required for abundance and subcellular localization of human CDC50 proteins and class 1 P4-ATPases. J Biol Chem 285:40088–40096

van Meer G, Voelker DR, Feigenson GW (2008) Membrane lipids: where they are and how they behave. Nat Rev Mol Cell Biol 9:112–124

Venter JC, Adams MD, Myers EW, Li PW, Mural RJ, Sutton GG, Smith HO, Yandell M, Evans CA, Holt RA, Gocayne JD et al (2001) The sequence of the human genome. Science 291:1304–1351

Vilsen B, Andersen JP, Clarke DM, MacLennan DH (1989) Functional consequences of proline mutations in the cytoplasmic and transmembrane sectors of the Ca^{2+}-ATPase of sarcoplasmic reticulum. J Biol Chem 264:21024–21030

Wach A (1996) PCR-synthesis of marker cassettes with long flanking homology regions for gene disruptions in *Saccharomyces cerevisiae*. Yeast 12:259–265

Waight AB, Pedersen BP, Schlessinger A, Bonomi M, Chau BH, Roe-Zurz Z, Risenmay AJ, Sali A, Stroud RM (2013) Structural basis for alternating access of a eukaryotic calcium/proton exchanger. Nature 499:107–110

Waugh DS (2005) Making the most of affinity tags. Trends Biotechnol 23:316–320

Weis BL, Schleiff E, Zerges W (2013) Protein targeting to subcellular organelles via MRNA localization. Biochim Biophys Acta 1833:260–273

West RW Jr, Yocum RR, Ptashne M (1984) *Saccharomyces cerevisiae GAL1-GAL10* divergent promoter region: location and function of the upstream activating sequence UASG. Mol Cell Biol 4:2467–2478

White SH (1998–2014) Membrane protein of 3D known structure, http://blanco.biomol.uci.edu/mpstruc/

Whorton MR, MacKinnon R (2011) Crystal structure of the mammalian GIRK2 K^+ channel and gating regulation by G proteins, PIP2, and sodium. Cell 147:199–208

Wildt S, Gerngross TU (2005) The humanization of N-glycosylation pathways in yeast. Nat Rev Microbiol 3:119–128

Zhang P, Toyoshima C, Yonekura K, Green NM, Stokes DL (1998) Structure of the calcium pump from sarcoplasmic reticulum at 8-A resolution. Nature 392:835–839

Zhang Z, Lewis D, Strock C, Inesi G, Nakasako M, Nomura H, Toyoshima C (2000) Detailed characterization of the cooperative mechanism of Ca^{2+} binding and catalytic activation in the Ca^{2+} transport (SERCA) ATPase. Biochemistry 39:8758–8767

Zimmermann R, Eyrisch S, Ahmad M, Helms V (2011) Protein translocation across the ER membrane. Biochim Biophys Acta 1808:912–924